NASA/CR-2000-208926

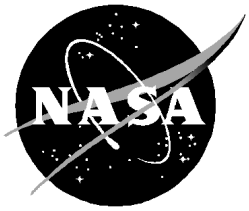

Purification Procedures for Single-Wall Carbon Nanotubes

Olga P. Gorelik
Pavel Nikolaev
Sivaram Arepalli

May 2001

The NASA STI Program Office . . . in Profile

Since its founding, NASA has been dedicated to the advancement of aeronautics and space science. The NASA Scientific and Technical Information (STI) Program Office plays a key part in helping NASA maintain this important role.

The NASA STI Program Office is operated by Langley Research Center, the lead center for NASA's scientific and technical information. The NASA STI Program Office provides access to the NASA STI Database, the largest collection of aeronautical and space science STI in the world. The Program Office is also NASA's institutional mechanism for disseminating the results of its research and development activities. These results are published by NASA in the NASA STI Report Series, which includes the following report types:

- TECHNICAL PUBLICATION. Reports of completed research or a major significant phase of research that present the results of NASA programs and include extensive data or theoretical analysis. Includes compilations of significant scientific and technical data and information deemed to be of continuing reference value. NASA's counterpart of peer-reviewed formal professional papers but has less stringent limitations on manuscript length and extent of graphic presentations.

- TECHNICAL MEMORANDUM. Scientific and technical findings that are preliminary or of specialized interest, e.g., quick release reports, working papers, and bibliographies that contain minimal annotation. Does not contain extensive analysis.

- CONTRACTOR REPORT. Scientific and technical findings by NASA-sponsored contractors and grantees.

- CONFERENCE PUBLICATION. Collected papers from scientific and technical conferences, symposia, seminars, or other meetings sponsored or cosponsored by NASA.

- SPECIAL PUBLICATION. Scientific, technical, or historical information from NASA programs, projects, and mission, often concerned with subjects having substantial public interest.

- TECHNICAL TRANSLATION. English-language translations of foreign scientific and technical material pertinent to NASA's mission.

Specialized services that complement the STI Program Office's diverse offerings include creating custom thesauri, building customized databases, organizing and publishing research results . . . even providing videos.

For more information about the NASA STI Program Office, see the following:

- Access the NASA STI Program Home Page at ***http://www.sti.nasa.gov***

- E-mail your question via the Internet to help@sti.nasa.gov

- Fax your question to the NASA Access Help Desk at (301) 621-0134

- Telephone the NASA Access Help Desk at (301) 621-0390

- Write to:
  NASA Access Help Desk
  NASA Center for AeroSpace Information
  7121 Standard
  Hanover, MD 21076-1320

NASA/CR-2000-208926

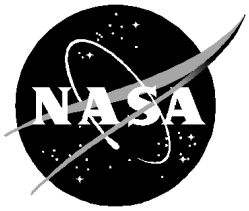

Purification Procedures for Single-Wall Carbon Nanotubes

Olga P. Gorelik
Pavel Nikolaev
Sivaram Arepalli
GBTech
NASA Johnson Space Center

National Aeronautics and
Space Administration

Lyndon B. Johnson Space Center
Houston, Texas 77058-4406

May 2001

Acknowledgements

We wish to acknowledge the support and encouragement from the JSC nanotube team members, especially Brad Files, William Holmes, Brian Mayeaux, and Carl Scott. Help from Benny Ewing, Lou Hulse, Dave Moore, and Glenn Morgan in the Building 13 laboratories is well appreciated. Thanks are also due to the Center for Nanoscale Science and Technology (CNST) group members and Chemistry Department of Rice University for providing access to their facilities. We are also grateful to Olga Shmakova of the University of Houston (UH) for NMR work and to Victor Hadjiev of Texas Center for Superconductivity (TCS), UH for Raman data. Finally, financial support for this GBTech-affiliated project has been received from NASA contract NAS 9-19100.

Contents

Acronyms

CNST	Center for Nanoscale Science and Technology
EDS	Energy-dispersive X-ray spectroscopy
HPLC	High performance liquid chromatography
NMR	Nuclear magnetic resonance
SEM	Scanning electronic microscopy
SWNT	Single-wall nanotube
TCS	Texas Center for Superconductivity
TEM	Transmission electron microscopy
TGA	Thermogravimetric analysis
UH	University of Houston
XRD	X-ray diffractometry

Purification Procedures for Single-Wall Carbon Nanotubes

Abstract

This report summarizes the comparison of a variety of procedures used to purify carbon nanotubes. Carbon nanotube material is produced by the arc process and laser oven process. Most of the procedures are tested using laser-grown, single-wall nanotube (SWNT) material. The material is characterized at each step of the purification procedures by using different techniques including scanning electron microscopy (SEM), energy-dispersive X-ray spectroscopy (EDS), transmission electron microscopy (TEM), Raman, X-ray diffractometry (XRD), thermogravimetric analysis (TGA), nuclear magnetic resonance (NMR), and high-performance liquid chromatography (HPLC). The identified impurities are amorphous and graphitic carbon, catalyst particle aggregates, fullerenes, and hydrocarbons. Solvent extraction and low-temperature annealing are used to reduce the amount of volatile hydrocarbons and dissolve fullerenes. Metal catalysts and amorphous as well as graphitic carbon are oxidized by reflux in acids including HCl, HNO_3 and HF and other oxidizers such as H_2O_2. High-temperature annealing in vacuum and in inert atmosphere helps to improve the quality of SWNTs by increasing crystallinity and reducing intercalation.

Goals

The main goal of this work is to find out the best technique to purify nanotube materials produced at Johnson Space Center by comparing two production techniques: laser oven and arc discharge. We use the term “nanotube material” or “product” instead of “nanotube” because nanotubes produced by every known technique so far contain various impurities. It is incorrect to refer to this mixture as “nanotubes,” which implies pure nanotubes. This report is centered on the purification of laser-produced material, since the quality of such materials is superior to arc-produced material and, therefore, requires less effort to purify. Other important goals are to gain an understanding of the kinds of impurities present with nanotubes before and after purification by various techniques, and possible chemical modification of nanorope and nanotube surfaces after purification.

Both arc and laser techniques are somewhat similar in the sense that carbon mixed with a small amount of metal catalyst is vaporized by either laser beam or arc discharge. Nanotubes self-assemble from vapor in the presence of catalysts. The laser oven technique is much better understood and allows more control over growth parameters (temperature, vapor concentration, and gas dynamics). Hence, the material quality is better.

Introduction

In the laser oven, a laser beam impinges on the carbon/catalyst target in an atmosphere of argon kept at 1473 K in the flow tube furnace. Temperature in the plume reaches 4000 to 5000 K. Carbon mixed with metal catalyst (typically 1:1 wt. % of Co: Ni) is vaporized and subsequently condenses into various products [1-5]. In addition to nanotubes, we see the formation of encapsulated metal particles, fullerenes [6], and amorphous carbon products [7]. Further analysis by NMR reveals the presence of polyaromatic and aliphatic hydrocarbons. EDS also shows small amounts of silicon. Various factors such as oven temperature, laser beam fluence, flow tube

geometry, and target composition and density affect nanotube quantity, purity, and, possibly, lengths and diameters [1,8,9]

In the arc discharge technique, a graphite anode drilled out and filled with a mixture of graphite powder and catalysts (typically 1:4 wt. % of Ni:Y) is vaporized in a direct current arc at 25-35 V and 100 A [10]. The chamber is filled with helium at ~650 kPa, and the temperature within the electric arc can reach 6000 K. During the burn process, a substance transfer occurs between the electrodes and nanotubes self-assemble from the vapor. In addition to nanotubes, carbon condenses into fullerenes, nanoparticles, and amorphous products. Organic impurities in the electrode material facilitate production of various hydrocarbons, which are revealed by NMR. The rate of the gas flow, size and orientation of the arc chamber, process scale, cooling system, the nature and purity of electrode materials, arc voltage, arc current and other factors affect the quantity, purity, and diameters of nanotubes produced. Localization of the resulting nanotube product in the arc chamber affects nanotube material properties as well. Nanotubes deposit in three distinct regions: collarette around cathode, webs that extend from collarette to chamber walls, and sooty deposit on the chamber walls. The best purity is obtained in the collarette material[10].

Characterization techniques

It is very important to be able to monitor material purity and kinds of impurities present at every stage of the purification process. No single technique can produce unambiguous answers and feedback, thus a number of different techniques were used to gain as much understanding as possible about our materials and processes.

a. SEM is the easiest tool. It provides medium-resolution images of the surface of nanotube material. It is possible to get a qualitative comparison of the purity of the samples [11], but it is sometimes not easy to distinguish nanotubes from the soot, especially when nanotubes are uniformly coated with impurities.
b. Our SEM is equipped with EDS. This allows seeing characteristic X-ray spectra of various elements and determining their atomic ratios in the sample. Unfortunately, concentrations of carbon are measured rather imprecisely.
c. TEM produces high-resolution images, but it is rather time-consuming. There are concerns about how representative of the whole sample the images are, since only a small fraction of the specimen can be looked at. It is easy to distinguish nanotubes from impurities and qualitatively compare the purity of the samples. Nanotube diameter distributions can be obtained from TEM pictures [12], which require a specially prepared specimen and take a lot of time.
d. XRD produces the lattice constant of a nanorope lattice. One can also see peaks from metal impurities and fullerenes. This is sensitive to the degree of crystallinity of the nanorope, which is affected by intercalation of impurities [1,11].
e. Raman spectroscopy produces characteristic peaks from certain phonon modes in nanotubes. Low-frequency ("breathing") modes at 150-200 cm^{-1} are dependent on nanotube diameters, but only resonant tubes show up [13]. It is impossible to get full information on the diameter distribution. The high-frequency (C-C stretch) mode at ~1585 cm^{-1} is sensitive to nanotube surroundings and can provide information on nanotube chemistry, although interpretation is ambiguous. The disordered carbon peak at ~1340 cm^{-1} is related to amorphous impurities as well as to disorder in nanotube walls.

f. TGA[1,14] is simply a measurement of specimen mass as its temperature slowly increases up to 800-1100°C. If done in inert gas (or vacuum), it shows that volatile compounds evaporate (certain hydrocarbons, fullerenes, etc.), leaving behind the fraction of non-volatile materials (typically nanotubes, metals, graphite, silicon, etc.) If done in air or oxygen, it shows temperatures at which nanotubes and impurities oxidize. The residual is then its ash content (typically metal oxides and silicon).
g. NMR was performed on solvent extracts of nanotube material. Any organic impurity produces proton peaks, whose positions are dependent on particular proton configuration; i.e., on the kind of steric group it is part of.
h. HPLC was performed on solvent extracts of nanotube material. It allows one to quantitatively determine the fraction of soluble fullerenes in the specimen. We hoped to determine other organic impurities, but poor performance of detector array in the ultraviolet region did not allow this. The HPLC apparatus at Rice University is equipped with a Cosmosil column for fullerene separation. There are reports that HPLC can also be used to separate nanotubes by length if used with a size-exclusion column [15].

Identification of impurities

EDS, SEM, and TEM proved the existence of inorganic impurities. Annealed samples of laser-produced material contain nickel, cobalt, and silicon. Nickel and yttrium found in arc material constitutes 10 to 20% by weight of the material total mass. Graphite-encapsulated catalyst metal (possibly carbide) particles were discovered and studied by means of SEM and TEM (fig. 1, 4d). EDS proves presence of metals, silicon, and carbon in the encapsulated particles. Figure 2 shows elemental maps of Si, Co, and Ni in the particle, which is wrapped in nanotubes. Figure 3 shows cumulative EDS spectra taken over approximately 20×30 μm area on the specimens, revealing the presence and relative intensities of Si, Co, and Ni peaks (Co and Ni are essentially removed in purified sample, Fig 3b, but this is not always necessarily the case).

XRD shows the presence of metals as well as fullerenes in samples (fig. 5).

TGA data (fig. 6) in argon flow clearly shows intense evaporation of water, volatile compounds and solvents at temperatures up to 200°C. Structures like -CH2-, -HC=CH-, $(C_6 H_x)_y$ evaporate in the temperature interval 200 to 250°C. Organic compounds evaporate at the temperature up to 450°C. Macromolecular compounds evaporate in the temperature interval up to 600°C. Fullerenes evaporate in the temperature interval 600 to 750 – 800°C. Decomposition of the material begins in the temperature interval 750 to 800°C or higher, and weight stabilizes in the interval 800 to 1200°C (fig. 6).

TGA can also be performed in air (or oxygen) flow. In this case, temperature has to be raised to the point of complete oxidation of carbon to determine the elemental composition of ash, inorganic materials, and their weight fractions.

Organic compounds and fullerenes were found by extracting raw materials with organic solvents: benzene, toluene, O-xylene, 1,2-dichlorobenzene, decaline, hexane, carbon disulfide, and other. An HPLC test of the solvent extract shows the presence of a full spectrum of fullerenes (C_{60}, C_{70}, C_{76}, C_{78}, C_{84}, C_{92}, C_{96}) and hydrocarbons (fig. 7). The amount of fullerenes extracted from raw nanotube material by toluene and benzene slowly increases on a time scale of several hours before it saturates at as much as 9% by weight (determined quantitatively by HPLC) (fig. 8). SEM images before and after extraction are essentially the same, indicating that many insoluble impurities are left in the sample (fig. 14). After extraction a sample typically

loses 18 to 20% of its mass. This allows us to estimate the amount of soluble hydrocarbons to be around 10% by weight.

NMR tests have determined the presence of H^+ in the extracted solutions. Localization of H^+ proves the presence of aromatic and linear hydrocarbons (fig. 9). Their weight fraction is 5 to 10% in accordance with the TGA data.

Raman peak in the area of 1340 cm^{-1} shows presence of amorphous carbon (figs. 10, 11).

We can conclude that typical laser material contains the following impurities by weight: Soluble fullerenes: ~10%. Total fullerenes content >10%, since some are insoluble. Soluble hydrocarbons: ~10%. Total hydrocarbons content >10%, since some are insoluble. Probably the total amount of fullerenes plus hydrocarbons is around 25 – 30%. Metal particle (catalyst): ~10%. Silicon: ~1 – 2%. The remaining 60 to 65% is divided among nanotubes, amorphous carbon, and graphitic shells surrounding nanoparticles. Half or more of that weight (30 to 35%) is probably nanotubes, and larger fraction of the rest is amorphous carbon. Therefore, approximate fractions of nanotube material components are:

Fullerenes: 12 – 15%
Hydrocarbons: 12 – 15%
Metals: ~10%
Silicon: ~1 – 2%
Amorphous carbon: ~20%
Graphitic shells: ~5 – 10%
Nanotubes: 30 – 35%

Purification methods and results

Raw material contains nanotubes, fullerenes, catalytic metal particles, amorphous carbon, and various kinds of hydrocarbons and their compounds. Oxidation by acids was used to remove catalytic particles, amorphous carbon, and hydrocarbons. The following techniques were tried on laser- and arc-produced material. Complete data on each sample and its particular treatment and analysis performed can be found in Tables 1 (laser) and 2 (arc). Data below centers on laser material.

1."Old Rice method"[1]. Oxidation by 5M nitric acid was performed over 24 hours at 96°C. The product was then neutralized by sodium hydroxide, suspended in 1% Triton X-100 surfactant solution in water, and purified by cross-flow filtration. It is difficult to dry nanotubes afterward, since vacuum evaporation does not work well because of foaming under vacuum, and non-vacuum evaporation is very slow. As a result of oxidization and neutralization, insoluble hydroxides of Ni and Co precipitate with nanotubes, heavy graphite particles, and organic Na salts which deposit into residue and are difficult to remove. Another big problem is that the 0.2 μm cross-flow filter cartridge is sufficiently permeable by nanotubes in Triton X-100 that a significant fraction of nanotubes is lost with the waste. At the same time, many particles are larger than the pore size and stay with the purified material (Fig. 12). Abundant quantities of nanotube are found in the waste, so it is not clear whether purified material is any purer than waste. This technique did not work well at all. The process is long and tedious, and results of cross-flow filtration are not reproducible.

2. The next method ("New Rice method"), recommended by Rice University, involved: oxidization by 5M nitric acid for 6 hours, centrifugation to separate the liquid (decant) from the heavy part, washing by water, neutralization by NaOH, secondary oxidization by nitric acid for 6 hours, separation by centrifugation, secondary neutralization by NaOH, washing by methanol, and redispersion in toluene. This technique is currently being used by Tubes@rice. The filtered toluene solution has a characteristic color of fullerene mixture. HPLC tests prove presence of C_{60}, C_{70} and higher fullerenes. Elemental analysis (EDS) of cleaned nanotubes shows a significant presence of catalytic metals, Na, and Si. TEM and SEM show encapsulated particles covered with amorphous carbon and nanoropes (i.e., nanotube bundles) covered by amorphous carbon (fig. 13). It is possible that the nanotube surface becomes derivatized with products of nitric acid reaction with amorphous carbon, judging by its look on high-resolution SEM images (Fig 26b). There is a lot of amorphous carbon left, which makes this technique a poor candidate. Nevertheless we can conclude that this technique is better than the former one ("Old Rice method"). Typical yield is 90 to 50%.

3. Solvent extraction followed by acid reflux. This method of purification starts with extraction of fullerenes and hydrocarbons with organic solvents: toluene, benzene, acetone, butanol, propanol, methanol, chloroform, decaline, ethyl ether, hexane, O-xylene, 1,2-dichlorobenzene, carbon disulfide, and some others. Solvent properties are tabulated in Table 4. SEM images of samples before and after extraction are presented in Figure 14. Since amorphous carbon and nanoparticles, which are the most visible on SEM, are unaffected by extraction the specimens look essentially the same. NMR spectra of extracts prove the presence of hydrocarbons (Figs. 7 a, b). Typically extraction removes 18 to 20% of the sample mass, out of which approximately half is soluble fullerenes (as determined by HPLC) and the rest are soluble hydrocarbons. There still may be some insoluble fullerenes and hydrocarbons left. Results of HPLC and NMR tests helped to choose the best solvents—toluene and benzene. Toluene, which is recommended due to its lower toxicity, was used in all of the following techniques. After extraction, the material was washed by methanol or acetone to remove the remains of the solvent used for extraction.

This was followed by oxidation by inorganic or organic acids. Inorganic acids tried were: HNO_3, HCl, mixture of HF and HNO_3, mixture of H_2SO_4 and HNO_3, $H_2S_2O_8$, H_2O_2. Organic acids tried were CH_3COOH, CF_3COOH, and CH_3COOOH. Acid properties are tabulated in Table 3. Acid oxidation was followed by washing of acid residue with hot water to a pH = 6 and then washing with methanol. Sometimes the neutralization was preformed with NaOH and/or NH_3OH.

3a. Nitric acid (HNO_3) was chosen because it is a strong oxidizer that is usually used for etching and oxidation of metals, but it is passive with respect to the surface of nickel and cobalt particles. HNO_3 reacts with non-metals and typical reducing agents. Since it is self-ionized in liquid form, the reaction is weak and, with increase in temperature, the acid dissociates into NO and NO_2 while the encapsulated catalytic particles stay intact. This sample was subjected to four subsequent refluxes in nitric acid. SEM images after each reflux are shown on Figure 15, and TEM images after the first and fourth reflux are shown on Figure 16 (the TEM image before purification can be found on Fig. 4d). Sample purity after the last reflux is not very good, there is still a significant quantity of amorphous carbon and nanoparticles (Fig. 16). Raman spectra (Fig. 10a) showed that C-C stretch peak normally positioned at 1585 cm^{-1} shifts to 1595 to 1605 cm^{-1} after the first reflux, which indicates a change in the local environment, possibly intercalation or

chemical derivatization with products of nitric acid reaction with amorphous carbon. The disordered carbon peak at 1360 cm^{-1} increases significantly after the first reflux, also indicating possible intercalation and disorder in nanotube walls. C-C stretch peak goes back to 1590 cm^{-1} and disordered carbon peak disappears upon drying at 150°C in air, indicating that intercalation mostly goes away. Similar results were observed by X-ray diffractomerty (Fig 5a). As-made material exhibits nanorope superlattice peaks, which are gone after reflux, indicating strong disorder and loss of crystallinity in nanoropes caused by intercalation. Upon drying nanoropes gain crystallinity back, indicating that intercalants are mostly removed. But since we continue to see impurities in electron microscopy images, this probably means that intercalants are not volatile enough to leave sample completely and rather redistribute on the surface of nanoropes. Typical yield is ~35%.

3b. The activity of HNO_3 increases with the addition of HF, which helps to dissolve Si compounds with the formation of NO, H_2O, and H_2 (SiF_6). The sample was first refluxed in concentrated HF for 30 min, then HNO_3 was added and the sample was refluxed further for 45 min at 35- to 40°C. Gas bubble release (H_2 and SiF_6) was observed. This technique has advantages for cleaning laser ablation material containing silicon. EDS spectra (Fig. 3b) shows that silicon is essentially removed. Nevertheless, other amorphous carbon impurities still exist in the sample (Fig.17). Typical yield is 40 to 80%.

3c. Hydrochloric acid (HCl) is one of the strongest oxidizers. It reacts with metals with negative and normal potential with release of H_2. It also reacts with metal oxides and hydroxides and generates free acids from silicates. SEM images are shown on Figure 18. Samples looked quite pure and the amorphous coating is mostly gone. The remaining coating swells with solution and is quite visible on SEM, but subsequent annealing (see below) demonstrates that the amount of coating is small. Typical yield is 70 to 90%.

3d. Sulfuric acid (H_2SO_4) is a strong acid but a weak oxidizer in diluted form. In concentrated form, it works as a strong oxidizer but passivates cobalt surfaces. It is difficult to find a working concentration of sulfuric acid that would accommodate the needs of purification. Separation of nanotubes and the decant is possible with multi-step dissolution of acid by methanol in separation funnel. Acid has high viscosity and is difficult to wash from nanotubes, so this technique was not pursued further. Typical yield is 30 to 40%.

3e. Peroxidisulfuric acid ($H_2S_2O_8$) is a strong oxidizer that reacts with organic compounds to full decomposition. Reaction was performed at room temperature with rapid outgassing until outgassing stopped in about 1.5 hrs. The viscosity of the acid is very high and separation of solid and liquid phase is difficult. Therefore, the same method as with H_2SO_4 was used. Solid and liquid phases are divided in separating funnel into different layers by adding methanol to the acid. The pure solid phase product contains encapsulated particles, but it usually does not contain amorphous carbon (Fig.19). It is possible that nanotubes were derivatized by products of reactions between the acid and amorphous carbons. Since both H_2SO_4 and $H_2S_2O_8$ catalyze the loss of water, there should not be any hydroxyl groups left. Typical yield is 25 to 45%.

3f. Hydrogen peroxide (H_2O_2) has oxidation-reduction properties, but the oxidizing function prevails because of the presence of O_2^-. The reaction was performed at 35°C for 3 hrs and is

accompanied by rapid release of CO (bubbles) and H_2O. After oxidation by H_2O_2 the material looks very good on SEM images (Fig. 20). The remaining amorphous coating swells with solution and is quite visible on SEM, but subsequent annealing (see below) demonstrates that the amount of coating is small. During the H_2O_2 oxidation of raw material, epoxy group formation on nanotube is possible. Typical yield 25 is 40%.

3g. Trifluoroacetic acid (CF_3COOH) is a strong acid that is used in organic synthesis as an oxidizer, a catalysis of electrophilic reactions, and a solvent of fluorine-containing compounds. The amount of silicon was distinctly lowered by the use of this acid. Also, the outer layer of the nanotubes looks smooth and clean (Fig. 21). The remaining coating swells with solution and is quite visible on SEM, but subsequent annealing (see below) demonstrates that the amount of coating is small. Typical yield is 60 to 80%.

3h. Peroxyacetic acid (CH_3COOOH) is another strong oxidizer of organic compounds. The reaction is very active with the rapid outgassing (CO); and formation of epoxy compounds, polycycles, and ethers is possible. This acid helps to break up large molecules and modify nanotube surface (Fig. 22a). These results were not particularly good. Typical yield is 80 to 90%.

4. High-resolution SEM microscopy shows that outer layer of nanoropes looks different after oxidation with different acids. Nevertheless, there is always a layer of the products of acid reaction with amorphous carbon and hydrocarbons present in the sample. These products are not completely soluble in the solvents used for washing after oxidation. Since these impurities no longer constitute non-volatile amorphous carbon but are chemical derivatives thereof, they may be volatile and can be evaporated away. In addition, some impurities can be evaporated away before acid reflux. Therefore, we have tried several techniques in which samples were subjected to high-temperature annealing in vacuum or argon flow before and/or after acid reflux. Vacuum annealing of laser material was performed at 1000° and 10 mTorr vacuum for 24 hrs whereas arc material was annealed at 800°C and 20 mTorr vacuum for 24 hrs. The typical weight loss was 60 to 90 %. Fullerenes and organic compounds condensed on cold surfaces at the exit of the tube furnace. SEM images show clean surfaces of nanoropes and clean encapsulated catalyst particles present inside aggregates. TEM images also show clean nanorope surfaces, and a small quantity of amorphous carbon present close to encapsulated catalyst particles. Ropes are well organized and seem to have a smooth surface and clear structure. Annealing was performed for 73 samples and each experiment produced good results (Figs. 23, 24).

4a. Simple Vacuum Annealing. Unpurified material was placed in the alumina boat in the vacuum furnace at 10 mTorr. Temperature was increased in 200°C steps to 1000°C over 20 hrs and then stayed at 1000°C for 4 hrs. There is definitely quite a lot of amorphous coating left on nanotube surface (Figs. 23a, b, d) that is not volatile even at such high temperature. Therefore, this technique is hardly suitable as a stand-alone purification method. It has to be combined with other steps (acid oxidation, solvent extraction). After annealing, a sample was studied by TGA in air flow up to 1000°C. At these conditions, nanotubes as well as amorphous coatings and graphitic particles oxidize and only metal oxides are left. The remaining weight fraction was ~54% of 1:1 CoO:NiO, which corresponds to about 35% by weight of Co and Ni. Specimen oxidation occurs at two distinct temperatures: ~430°C and ~550°C. Some publications believe that these temperatures correspond to oxidation of amorphous carbons (first peak) and nanotubes

(second peak). It is also possible that the first peak corresponds to oxidation of amorphous carbon and the nanotube layer to which it adheres. The peak areas are about the same, which means that there are at least equal amounts of nanotubes and amorphous deposits.

4b. Technique 3a (toluene extraction + HNO_3 reflux) was followed by annealing in argon flow up to 1100°C (Fig. 24). Annealing was performed in TGA, and the specimen mass was monitored as the temperature was increased in 200°C steps (Fig. 24d). The sample has lost at least 50% of its mass and looks very good on SEM and TEM images. Nanoropes are well-formed and crystalline. Amount of amorphous coating is minimal, but there are still some nanoparticles left in the sample. Typical yield is 80 to 90% after extraction and ~50% after reflux.

4c. Technique 3c (toluene extraction + HCl reflux) was followed by annealing in vacuum for 24 hrs. up to 1000°C at 10 mTorr as temperature was increased in 200°C steps. The sample looks very good on SEM images (Fig. 25). After vacuum annealing, the sample was studied in TGA in air flow up to 800°C (Fig. 25d). At this condition, nanotubes as well as the amorphous coating and graphitic particles oxidize. All that are left are metal oxides. The mass left after burning all nanotubes and carbon-containing dirt was ~33%, which corresponds to ~25% metals by weight. One can distinguish 3 peaks on the dm/dt curve, the first at 420°C, the second at 480°C, and the third at 550°C. The first and third peak positions are quite similar to that of technique 4a, but the peaks are broader and there is another peak in between those two. The first peak area is about equal to the total area of the second and third peaks. Overall, this technique gave excellent results. Typical yield is 80 to 90% after extraction and ~70% after reflux.

4d. A set of samples was annealed in vacuum for 24 hrs up to 1000°C at 10 mTorr as the temperature was increased in 200°C steps. Afterward all these samples were refluxed in various acids to observe how particular acids affect nanotube surfaces after annealing. The main goal here was the study of nanotube surface behavior rather than purification per se. Acids tried include CH_3COOOH, HNO_3, H_2O_2, and $H_2S_2O_8$.

The surface looks quite different after reflux in different acids (Fig. 26). Note that all images are taken at the same magnification, but the visible nanorope diameter is different, which means that the nanorope coating adsorbs hydroxyl groups from the acid and intake is different for different acids. Nanoropes look quite similar after peroxyacetic and persulphuric acids reflux. They have smooth surfaces and less swelling. After hydrogen peroxide reflux, the nanoropes swelled a lot more, and the surface is smooth and somewhat fuzzy. After nitric acid reflux, nanoropes do not swell much and the surface is grainy. These results clearly show that acid reflux results in modification of amorphous coating on nanoropes, and this modification varies significantly for different acids. It is also possible that nanotubes themselves are derivatized to a different degree, but we cannot confirm it experimentally.

It is interesting that the swelling of nanoropes is reversible. One of the samples was studied in TGA after reflux in H_2O_2 (Fig. 27c). Annealing was performed in TGA in argon flow and the specimen mass was monitored as the temperature was increased in 200°C steps to 1100°C. Approximately 66% of the sample mass was left, indicating that there is only 34% by weight of volatile compounds. The sample looks very clean after annealing, and the swelling is gone.

Some of these samples were checked by Raman spectroscopy (Fig. 11). In particular, samples refluxed in CH_3COOOH (no. 4), $H_2S_2O_8$ (no. 5), and H_2O_2 after TGA (no. 6). Those can

be compared with the unpurified sample (no. 8) and one only annealed before reflux (no. 7). The C-C stretch peak position is located at 1588 cm^{-1} in unpurified and annealed samples; yet it shifts significantly after refluxes, indicating a change in the local environment of nanoropes. This may include charge transfer from amorphous coating reacting with acids and/or direct nanotube derivatization. The shift is largest for CH_3COOOH reflux, somewhat smaller for $H_2S_2O_8$ reflux, and even smaller for H_2O_2 reflux + annealing, which may be due to partial removal of intercalants during annealing.

4e. A set of samples after vacuum annealing (24 hrs up to 1000°C at 10 mTorr as temperature was increased in 200°C steps) was dispersed in various organic solvents. The main goal here was also the study of nanotube surface behavior and nanotube dispersion rather than purification per se. Solvents tried were: carbon disulfide, dimethylformamide, water, hexane, propanol, toluene, dimethylsulfoxide, cyclohexane, and some others (Figs. 28, 29). Nanotubes behave very differently in different solvents. Amorphous coatings on nanorope surfaces adsorb solvents and swell to different degrees, possibly forming solvates. Dimethilsulfoxide and cyclohexane cause the least swelling, whereas propanol and hexane swell more, and toluene and dimethylformamide swell the most. Carbon disulfide and water hardly produce any swelling. It looks like carbon disulfide causes coagulation of the amorphous coating on the nanorope surface. Water may introduce hydroxyl groups into the coating, which may adsorb or chemically react with it. Note that all SEM images are again taken at the same magnification.

Comments on nanotube behavior

After nanotubes and amorphous carbon are dissolved in methanol, ethanol, ether, and other solvents, they have a porous and flocculent structure that shows very well on SEM and TEM photographs.

After oven drying for a long time, the weight stabilizes. This shows that the material has a porous structure and adsorbs water and gases from the air.

When dried material is placed into a solvent (methanol, acetone, water, etc.) for about an hour, we observe a well-pronounced swelling. The sample volume increases 5 to 10 times and assumes a gel-like structure. In SEM, the material has a very smooth structure that does not scatter electrons well.

In solvents, nanotubes and their aggregates behave like colloidal solutions. Upon precipitation or solution thickening by evaporation, the nanotubes form flocks with properties of a sol. Upon dilution and dispersion of these solutions, nanotubes form aggregates of small particles that behave like micells taking part in Brownian motion. It appears that each aggregate has a surface charge, since – as particles collide with each other in Brownian motion – the particle size increases and coagules grow.

The coagulation process is affected by factors such as particular type of solvent, temperature, and electrostatic forces when initial aggregates collide with each other in Brownian motion or in directional motion in electrostatic field, or when solution is physically agitated.

Initial aggregates are bound directly by intermolecular forces. The interaction of solvents (methanol, ether, acids, etc.) with amorphous carbon localized on and intimately bound to the nanorope surface partially solvates carbon and, possibly, some nanotubes in the outer layer of the nanorope. This leads to interactions through the layer of solvate.

Upon nanotube dispersion in any solvent, we observe that the system is unstable thermodynamically on several time scales:

- The first period, which is on the order of 1 to 5 days, is characterized by flocculation and formation of sol.
- The second period, which is on the order of 3 to 20 days, is characterized by coagulation and an increase in particle size.
- The third period, which is on the order of 10 to 40 days, is characterized by the coalescence of aggregates and particles. It appears that particles grow as material from other particles dissolves and/or changes phase state and then add to other particles in other phase states.

A good proof that nanotubes coalesce is the observation of nanotube suspension behavior upon centrifugation of the products of acid oxidation. Nanotubes form decants which, after neutralization and drying, form solid films rich in nanotubes. Nanotubes in the film are in form of fairly thick nanoropes, or fibers, which can be packed in various fashions.

General comments and future work

Material produced by laser ablation contains fullerenes, and a higher fullerene concentration usually means cleaner raw material, which has more nanotubes. The presence of silicon in the laser material was observed by elemental analysis (EDS). The arc material does not contain silicon, but the quality and quantity of nanotubes in the arc material is lower than in laser ablation material. It was observed that, in laser-produced nanotubes, purity correlates with silicon content. The smaller silicon content corresponds to lower purity. Silicon may, therefore, be a factor that affects the quality and quantity of nanotubes formed by either of the processes. But since no systematic studies were performed, this is only a hypothesis.

It is speculated that amorphous carbon localized around encapsulated catalyst particles, and which we try to get rid of in the purification process, can possibly be the building material of nanotubes. This may yield the possibility of nanotube growth in “nutrient media” at room temperature and atmospheric pressure.

In further studies of the properties of nanotubes, it will be important to include new diagnostic techniques including: IR and UV-visible spectra, mass spectrometry, and NMR spectra. A comprehensive study should show additional properties of nanotube materials. These tests will be useful for functional synthesis and will also help to find better ways to purify raw material. In future, these methods could be electrostatic purification in gas flow or electrolysis in liquid.

Conclusions about purification techniques

Of about 50 samples of laser material and 67 samples of arc material – all of which were produced by laser or arc techniques at equal or almost equal conditions, respectively – the variations in properties of the materials were quite large.

The results of purification show the following trends. Incorporation of dry steps (annealing) into purification methods generally produces better results. Hydrocarbons and fullerenes evaporate in the processes of high-temperature annealing, after which the outer layer of the nanoropes is much cleaner and does not contain much amorphous material. Encapsulated catalyst particles are not covered by amorphous carbon, while a significant amount of amorphous

carbon is found on the surface of nanoropes close to encapsulated particles, where the nanoropes interlace the most. This first step can be replaced with toluene extraction, which also removes soluble fullerenes and hydrocarbons. Nevertheless, annealing looks more promising as a first step, since it can also disrupt graphitic shells on metal particles and facilitate subsequent metal removal.

Subsequent oxidation by hydrochloric acid or hydrogen peroxide helps to remove some of the remaining amorphous coating and makes the rest more susceptible to vaporization, so that it can be removed in the second vacuum annealing. The most promising techniques, therefore, are 4c and 4d (H_2O_2 or HCl oxidation). 4c (HCl oxidation) generally produces higher yields.

Annealing as a last purification step also improves the crystallinity of nanoropes and helps to get rid of intercalants introduced into inter-tubular spaces by acid reflux. Nitric acid reflux on any step gives inferior results to H_2O_2 or HCl. All acid oxidation methods probably cause either dissolution of the nanotube walls or addition of different radicals and/or compounds to the surface of nanotubes. This results in radicals on nanorope surfaces, which are difficult to remove by vacuum annealing at temperatures up to 1000 C. Nitric acid is probably the worst in this sense, giving nanorope coatings that are more difficult to remove.

References

1. A. G. Rinzler, J. Liu, H. Dai, P. Nikolaev, C. B. Huffman, F. J. Rodriguez-Marcias, P. J. Boul, A. H. Liu, D. Heymann, D. T. Colbert, R. S. Lee, J. E. Fischer, A. M. Rao, P. C. Eklund and R. E. Smalley, "Large-scale purification of single-wall carbon nanotubes: process, product and characterization," *Applied Physics A* **67**, pp. 29-37 (1998).
2. S. Arepalli, P. Nikolaev, W. Holmes, and C. D. Scott, "Diagnostics of laser produced plume under carbon nanotube growth conditions," *Applied Physics A* **70**, pp. 125-134 (2000).
3. E. Munoz, W. K. Maser, A. M. Benito, M. T. Martinez, G. F. de la Fuente, A. Righi, J. L. Sauvajol, E. Anglaret, and Y. Maniette, "Single-walled carbon nanotubes produced by cw CO_2-laser ablation: study of parameters important for their formation," *Applied Physics A* **70**, pp. 145-151 (2000).
4. M. Yudasaka, F. KoKai, K.Takahashi, R.Yamada, N.Sensui, T.Ichihashi, anS.Iijima, "Formation of single-wall carbon nanotubes: comparison of CO_2 laser ablation and Nd:YAG laser ablation", *Journal of Physical Chemistry B* **103**, pp. 3576-3581 (1999).
5. A. C. Dillon, P. A. Parilla, J. I. Alleman, J. D. Perkins, and M. J. Heben, "Controlling single-wall nanotube diameters with variation in laser pulse power," *Chemical Physics Letters* **316**, pp. 13-18, (2000).
6. B. W. Smith, M. Monthioux, and D. E. Luzzi, "Carbon nanotube encapsulated fullerenes: a unique class of hybrid materials," *Chemical Physics Letters* **315,** pp. 31-36, (2000).
7. T. Ishigaki, S. Suzuki, H. Kataura, W. Kratschmer, and Y. Achiba, "Characterization of fullerenes and carbon nanoparticles generated with a laser-furnace technique," *Applied Physics A* **70**, pp. 121-124 (2000).
8. O. Jost, A. A. Gorbunov, W. Pompe, T. Pichler, R. Friedlein, M. Knupfer, H.-D. Bauer, L. Dunsch, M. S. Golden, and J. Fink, "Diameter grouping in bulk samples of single-walled carbon nanotubes from optical absorption spectroscopy," *Applied Physics Letters* **75**, pp. 2217-2219 (1999).

9. M. Yudasaka, R. Yamada, N. Sensui, T. Wilkins, T. Ichihashi, and S. Iijima, “Mechanism of the effect of NiCo, Ni and Co catalysts on the yield of single-wall carbon nanotubes formed by pulsed Nd:YAG laser ablation,” *Journal of Physical Chemistry B* **103**, pp. 6224-6229 (1999).
10. C. Journet, W. K. Maser, P. Bernier, A. Loiseau, M. Lamy de la Chapelle, S. Lefrant, P. Deniard, R. Lee, and J. E. Fischer, “Large-Scale Production of Single-Walled Carbon Nanotubes By the Electric-Arc Technique,” *Nature* **388**, pp. 756-758 (1997).
11. A. Thess, R. Lee, P. Nikolaev, H. Dai, P. Petit, J. Robert, C. Xu, Y. H. Lee, S. G. Kim, A. G. Rinzler, D. T. Colbert, G. E. Scuseria, D. Tománek, J. E. Fischer, and R. E. Smalley, “Crystalline Ropes of Metallic Carbon Nanotubes,” *Science* **273**, pp. 483-487 (1996).
12. P. Nikolaev, A. Thess, A. G. Rinzler, D. T. Colbert, and R. E. Smalley , “Diameter doubling of single-wall nanotubes,” *Chemical Physics Letters* **266**, pp. 422-426 (1997).
13. M. A. Pimenta, A. Marucci, S. D. M. Brown, M. J. Matthews, A. M. Rao, P. C. Eklund, R. E. Smalley, G. Dresselhaus, and M. S. Dresselhaus, “Resonant Raman Effect in Single-Wall Carbon Nanotubes,” *Journal of Materials Research*, **13**, pp. 2396-2404 (1998).
14. A. Dillon, T. Gannett, K. Jones, J. Alleman, P. Parilla, and M. Heben, “Simple and complete purification of single-walled carbon nanotube materials,” *Advanced Materials* **11**, pp. 1354-1358 (1999).
15. G. S. Duesberg, J. Muster, V. Kristic, M. Burghard, and S. Roth, “Chromatographic size separation of single-wall carbon nanotubes,” *Applied Physics A* **67**, pp. 117-119 (1998).

Appendix A

Tables and Figures

Tables and Figures

Table 1. Complete data on purification of laser-made nanotube material.

Sample #	Extraction	Washing	Sublimation	Reflux	Neutralization	Washing	Dry	Annealing	Testing	Weigh
5				2/HNO3		H2O	air	annealing	SEM	
5 decante film after 1st step				H2S2O8	H2O/MeOH	MeOh	air		SEM, EDS	
5decant film after 1st step								vac.1000C	SEM,EDS	0.0011/0.0005
5								vac.1000C	SEM.EDS	0.0154/0.0042
10(9517)				2/HNO3	NaOH	MeOH/Toluene	air		SEM,Raman	0.09517/0.04180
10(8305)	Toluene	MeOH		HNO3		H2O/MeOH	ai/oven		SEM,Raman	0.08305/0.0588
10(8535)	Toluene	MeOH/dry	14hours/	HNO3	H2O/MeOH	Toluene/MeOH	air/oven		SEM,Raman	0.08535/0.02934
10(7761)	Acetone/Tolue	MeOH/dry		HNO3♣	NaOH/H2O	MeOH	air/oven		SEM,Raman	0.07761/0.05480
10(5536)		Acetone	26hours							
10				2/HNO3	NaOH	MeOH/Toluene	air		SEM	0.5964/0.3079
18				4/HNO3		H2O/MeOH	air		SEM,TEM,Raman,X-ray	0.6296/
18	Toluene	MeOH/Acetone		2/HNO3		H2O/MeOH	air		HPLC,SEM	.0507/.04113/.023
18	Benzene	MeOH/Acetone		2/HNO3		H2O/MeOH	air		HPLC,SEM	.051/.0471/.03028
18		Acetone	9hours/1180F	1/HNO3		H2O/MeOH	air/dry		SEM,TEM	.1267/.0881/.0613
18	Toluene	MeOH		2/HNO3	NaOH/Triton100X	H2O	air			0.1914
18	Toluene		1000C,Vac					annealing		
18		MeOH	1000C,Vac					annealing		0.0115/0.0116
18			1000C,Vac					annealing		0.0127/0.0041
18	Toluene	MeOH	1000C,Vac					annealing		0.0159/0.0144
18	crfl			H2S2O8	MeOH/H2O	MeOH	air		SEM	
18	crfl, H2S2O8							vac.1000C	SEM, EDS	0.037/0.02085
19				2/HNO3	NaOH	MeOH/Toluene	air/oven		SEM,TEM,Raman	1.0179/0.1760bp
19 waste	after 1st step			H2O2+H2S2O8	MeOH on separ.fannel				SEM,EDS	/0.00735
29								annealing/air	SEM	0.04964/0.0087
29	Toluene	MeOH		HCl	NaOH/H2O	MeOH			SEM	0.4238/
29	ext,HCl reflax							vac.1000C	SEM,EDS	0.2504/0.035
29	Toluene	MeOH					dry		SEM, EDS	/0.150/ 0.1244
29	ext,dry							vac.1000C	SEM,EDS	0.0372/0.0088
15	Toluene	MeOH		2/HNO3		H2O/MeOH	air		SEM,EDS	0.0514/
15	Toluene	MeOH/NaOH		HNO3	hot H2O	MeOH			SEM,EDS	0.8283/ 0.4135
11	Toluene	MeOH		HNO3	hot H2O				?	0.5973/
11 water decante								vac.1000C		/0.0099
11	after purification							vac.1000C	SEM,EDS	3.174wet/0.40334

Table 1. Complete data on purification of laser-made nanotube material. (Continued)

Sample #	Extraction	Washing	Sublimation	Reflux	Neutralization	Washing	Dry	Annealing	Testing	Weigh
2	Toluene	MeOH						annealing/air	SEM,EDS	0.2566/0.0403
2	after 1st step			H2S2O8	MeOH/H2O	MeOH			SEM,EDS	
2			400C, air					annealing/air	SEM,EDS	0.2536/ 0.031
7	Toluene	MeOH		HF/HNO3	hot H2O	MeOH			SEM,EDS	0.6097/
7								vac. 1000C	SEM,EDS	0.0946/0.0487
8	Toluene	MeOH		HNO3	hot H2O	MeOH			SEM, EDS	0.5246/
16	Toluene	MeOH		HNO3	hot H2O/NaOH	MeOH	redisNaOH		SEM, EDS	1.0088/
16	Toluene	MeOH		H2S2O8	MeOH/H2O	MeOH	oven/air		SEM, EDS, Raman	0.0507/0.0277
16	Toluene	MeOH		H2O2	vac.filtr/ MeOH	MeOH	oven/air		SEM,EDS, Raman	0.0524/0.0198
16	Toluene	MeOH		CF3COOH	Na2CO3	H2O	oven/air		SEM, EDS, Raman	0.0639/0.0646
16	after purification by CF3COOH			H2O2+H2SO4	MeOH participation on sep. fannel				SEM, EDS, Raman	0.0640/0.4110
16waste	after HNO3			CH3CO3H	MeOH				SEM, EDS, Raman	/0.1208
16	Toluene	Ethyl Ether							SEM,EDS, Raman	0.0466/0.04080
16	after H2S2O8							vac. 1000C	SEM, EDS, Raman	0.0277/0.01707
16	after H2O2							vac. 1000C	SEM,EDS, Raman	0.0198/0.01390
16	after HF3COOH	& H2O2+H2SO4						vac. 1000C	SEM,EDS, Raman	0.0411/0.02806
16?								vac. 1000C	SEM,EDS, Raman	0.03802/0.034
17	Toluene	MeOH		HNO3	hot H2O/NaOH	MeOH	redisNaOH		SEM, EDS	0.8622/
17	after 1st step			H2S2O8	MeOH/ H2O	MeOH			SEM, EDS, Raman	
17	after 2nd step							vac. 1000C	SEM, EDS,	0.11681/0.07844
17	after HNO3							vac. 1000C	SEM,EDS	0.18363/0.10835
17	after HNO3	magnite						vac. 1000C	SEM,EDS	0.20232/0.11918
22	Toluene	MeOH		HCl	hot H2O/NaOH	MeOH			SEM, EDS ???	0.631/
22	after HCl purification							vac. 1000C	SEM,EDS,Raman	0.4228/0.1639
22	Toluene	MeOH					dry		SEM, EDS	/0.1836/.1717
22	ext.,dry							vac.1000C	SEM,EDS,Raman,MS	0.0703/0.0234
22								vac.1000C	SEM,EDS,Raman,MS	0.00139/0.00051
22								vac.1000C	SEM,EDS,Raman	0.1140/0.0864
22	after vac annealing			H2S2O8	MeOH		air		SEM,EDS,Raman	0.0028/0.00144
22	after vac annealing			CH3CO3H	MeOH		air		SEM,EDS,Raman	0.0024/0.001214
22	after vac annealing			H2O2			air		SEM,EDS,Raman	0.0082/0.00311
22	after vac annealing			HNO3	MeOH		air		SEM,EDS,Raman	
22	after vac annealing					Hexane			SEM,EDS,TEM,Raman	

Table 1. Complete data on purification of laser-made nanotube material. (Continued)

Sample #	Extraction	Washing	Sublimation	Reflux	Neutralization	Washing	Dry	Annealing	Testing	Weigh
22	after vac annealing					MeOH			SEM,EDS,TEM,Raman	
22	after vac annealing					PrOH			SEM,EDS,TEM,Raman	
22	after vac annealing					Toluene			SEM,EDS,TEM,Raman	
22	after vac annealing					DMF			SEM,EDS,TEM,Raman	
22	after vac annealing					H2O			SEM.EDS,TEM,Raman	
22	after vac annealing					NaOH			SEM,EDS,TEM,Raman	
22	after HCl,Annealing					Chloroform			SEM,EDS,Raman	
22	after HCl,Annealing					O-xylene			SEM,EDS,Raman	
22	after HCl,Annealing					Acethyl Acetone			SEM,EDS,Raman	
22	after HCl,Annealing					Pyridine			SEM,EDS,Raman	
22	after HCl,Annealing					Phenol Phthalene			SEM,EDS,Raman	
22	after HCl,Annealing					Dimethyl Sulfoxide			SEM,EDS,Raman	
22	after HCl,Annealing					Cyclohexane			SEM,EDS,Raman	
22	after HCl,Annealing					DFM			SEM,EDS,Raman	
22	after HCl,Annealing					MEK			SEM,EDS,Raman	
22	after HCl,Annealing					Decaline			SEM,EDS,Raman	
22	after HCl,Annealing					CS2			SEM,EDS,Raman	
49								vac.1000C	SEM,EDS	0.0199/0.0504
49(1"tube)								vac.1000C	SEM,EDS	0.0129/0.00506
49(film)								vac.1000C	SEM,EDS	/0.00211
1R (1st)								vac.1000C	SEM,EDS	
1R(2nd)								vac.1000C	SEM,EDS	
1R(3rd)								vac.1000C	SEM,EDS	
2R(1st)								vac.1000C	SEM,EDS	
2R(2nd)								vac.1000C	SEM,EDS	
2R(3rd)								vac.1000C	SEM,EDS	
20	Toluene	MeOH		HNO3	hot H2O	MeOH				0.8203/
20	Toluene	MeOH		HF/HNO3	hot H2O	MeOH	air/dry		SEM	0.0196/
20				plasma ache					SEM,EDS, IR	0.02265/
20	after HNO3			plasma ache					SEM,EDS, IR	0.05488/
29/2								vac.1000C	SEM,EDS	0.72371/0.653
29/2	after annealing			H2O2			air		SEM,EDS	0.2413/0.2299
29/2	after annealing			CH3COOH			air		SEM,EDS	0.3697/0.3980

Table 1. Complete data on purification of laser-made nanotube material. (Concluded)

Sample #	Extraction	Washing	Sublimation	Reflux	Neutralization	Washing	Dry	Annealing	Testing	Weigth
44								vac.1000C	SEM,EDS	0.40514/03516
44	after annealing			HCl	MeOH		air		SEM,EDS	0.0108/0.0114
44	after annealing			CH3COOH	MeOH		air		SEM,EDS	0.0109/0.0115
44	after annealing			H2O2	MeOH		air		SEM,EDS	0.0109/0.0042
44	after annealing			CH3CO3H	MeOH		air		SEM,EDS	0.0125/0.0135
44	after annealing			CF3COOH	MeOH		air		SEM,EDS	0.0122/0.0148
44	after annealing			HNO3	MeOH		air		SEM,EDS	0.0175/0.0126
44	after annealing			H2S2O8	MeOH		air		SEM,EDS	0.0179/0.0055
44	after annealing			HF+HNO3	MeOH/H2O		air		SEM,EDS	0.0174/0.0195
44	after annealing									
44	after annealing									
44	after annealing									
44	after annealing									
44	after annealing									
44	after annealing									
44	after annealing	Toluene							SEM.EDS	~3mg
44	after annealing	ODB							SEM.EDS	~3mg
44	after annealing	Chloroform							SEM.EDS	~3mg
44	after annealing	Pyridine							SEM.EDS	~3mg
44	after annealing	DMF							SEM.EDS	~3mg
44	after annealing	MEK							SEM.EDS	~3mg
44	after annealing	Cyclohexane							SEM.EDS	~3mg
44	after annealing	Hexane							SEM.EDS	~3mg
44	after annealing	O-xylene							SEM.EDS	
44	after annealing	Decaline							SEM.EDS	
44	after annealing	Acethyl Acetone							SEM.EDS	
44	after annealing	Dimethylaniline							SEM.EDS	
44	after annealing	Dimethyl Sulfoxide							SEM.EDS	
44	after annealing	THF							SEM.EDS	
44	after annealing	CS2							SEM.EDS	
44	after annealing	Benzene							SEM.EDS	
44	after annealing	CCl4							SEM.EDS	
44	after annealing	CH2Cl2							SEM.EDS	

Table 2. Complete data on purification of arc-made nanotube material.

##	Sample #	Extraction	Washing	Sublimation	Reflux	Neutralization	Washing	Dry	Annealing	Testing
1	5coll				2/HNO3		H2O	air	annealing	
2	5dep									
3	17coll				2/HNO3	NaOH	MeOH/Toluene	air		
4	17dep				HNO3	cross-flowNaOH	H2O/MeOH	air		
5	19coll								vacuum 1000C	SEM, EDS
6	19dep								vacuum 1000C	SEM, EDS
7	24coll		NaOH/hot H2O		HF/HNO3	H2O	H2O/MeOH	air/oven		EDS,SEM
8	24coll								vacuum 1000C	EDS,SEM
9	25coll		NaOH/hot H2O		HF/HNO3	H2O	H2O/MeOH	air/oven		EDS,SEM
10	25coll								vacuum 1000C	SEM, EDS
11	37coll				2/HNO3	NaOH	H2O/Acetone	air		EDS,SEM
12	37dep				2/HNO3	NaOH	H2O/Acetone	air		
13	38coll								vacuum 1000C	SEM, EDS
14	38coll	Toluene	MeOH		HF/HNO3	H2O	H2O/MeOH	air/oven		EDS,SEM
15	38dep				2/HNO3	NaOH				
16	50coll									
17	50dep									
19	51coll									
20	51dep									
21	52coll	Toluene	MeOH/NaOH		HNO3	H2O	H2O/MeOH	air		HPLC,EDS,SEM
22	52dep	Toluene	MeOH/NaOH		HNO3	H2O	H2O/MeOH	air		HPLC,EDS,SEM
23	52coll	Benzene	MeOH/NaOH		HNO3	H2O	H2O/MeOH	air		HPLC,EDS,SEM
24	52dep	Benzene	MeOH/NaOH		HNO3	H2O	H2O/MeOH	air		HPLC,EDS,SEM
25	53coll	Toluene	MeOH/NaOH		HNO3	H2O	H2O/MeOH	air		HPLC,EDS,SEM
26	53dep	Toluene	MeOH		2/HNO3	H2O	H2O/MeOH	air		HPLC,EDS,SEM
28	53coll	Benzene	MeOH/NaOH		HNO3	H2O	H2O/MeOH	air		HPLC,EDS,SEM
29	53dep	Benzene	MeOH		2/HNO3					
30	52coll		Acetone	vacuum/temp.						EDS,SEM

Table 2. Complete data on purification of arc-made nanotube material. (Concluded)

##	Sample #	Extraction	Washing	Sublimation	Reflux	Neutralization	Washing	Dry	Annealing	Testing
42	26coll								vacuum 1000C	SEM, EDS
43	26dep									
44	39coll								vacuum 1000C	SEM, EDS
45	39dep									
46	48coll								vacuum 1000C	SEM,EDS
48	48dep									
49	72coll	Toluene	MeOH		2HNO3	H2O/ NaOH	hot H2O	air/oven		SEM, EDS, TGA, Raman
50	72dep									
51	73coll	Toluene	MeOH		2HNO3	H2O/ NaOH	hot H2O	air/oven		SEM, EDS, Raman
52	73dep									
53	72coll		Acetone						air 600	SEM,EDS
54	72coll	after line 51							air 600	SEM,EDS
55	72coll				H2O2				vacuum1000	SEM,EDS
56	72coll				H2S2O8				vacuum1000	SEM,EDS
57	72coll				CF3COOH				vacuum1000	SEM,EDS
58	72coll		Ethyl Ether						vacuum1000	SEM,EDS
59	73coll		Acetone						air 600C	SEM,EDS
60	73coll	after line 54							air 600C	SEM,EDS
61	73coll		Ethyl Ether						vacuum 1000C	SEM,EDS
62	37coll(dec)								vacuum 1000C	SEM,EDS, TEM,Raman, IR
63	37dep								vacuum1000C	SEM,EDS

Table 3. Properties of organic and inorganic acids.

##	Name (abbrev.)	Formula	Mol.Wt.	B.p. oC	M.p. oC	density,	diel.const	refraction	b.moment	viscosity
1	Nitric acid	HNO3	63.01	82.6	-41.6	1.504	1.397		2.17	8.9
2	Hydrochloric acid	HCl								
3	Hydrofluiric acid	HF	20.01	19.51	-89.4	1.123(-50)	1.1574	84	1.82	2.4
4	Sulific acid	H2SO4	98.08	305	10.371	1.827		101		245
5	Pyroxodisulific acid	H2S2O8		184		1.9				
6	Hydrogen Peroxide	H2O2	34	150	-0.41	1.442		84.2	2.2	
7	Trifluoroacetic acid	CF3COOH	114.02	72.4	-15	1.54		39	2.28	5.78
8	Pyroxiacetic acid	CH3COOOH								
9	Acetic acid	CH3COOH	60.1	118	17	1.049		6.15		
10	Propionic acid	CH3CH2CO2H	74.1	141	-21	0.993				
11	Formic acid	HCO2H	46	101	8.3	1.22				

Table 4. Properties of organic solvents.

##	Name (abbrev.)	Formula	Mol.Wt.	B.p. C	M.p.C	density,	diel.const	refraction	b.moment	viscosity
1	Acetone	CH3COCH3	58.08	56.2	-95.4	0.79	1.3588	20.7	2.88	3.16
2	Methanol	CH3OH	32	65	-98	0.791	1.3288	32.7	1.7	5.45
3	Propanol	C3H7OH	60.11	82.4	-89.5	0.786	1.3776	18.3	1.66	17.7
4	Butanol	C4H9OH	74.12	99	-115	0.806	1.3978	15.8	1.7	42.1
5	Ethyl Ether	(C2H5)2O	74.12	34.5	-116	0.714	1.3526	4.34	1.15	2.22
6	Hexane	C6H14	86.18	69	-95	0.66	1.3751	1.89	0.08	2.92
7	Methyl Ethyl Keton	CH3COC2H5	72.12	79.6	-86	0.805	1.3788	18.5	2.5	36.5
8	Carbon Disulfid	CS2	76.1	46	-112	1.27	1.6319	2.64	0	3.76
9	NN-Dimethyl Formamid (DMF)	HCON(CH3)2	73.1	152	-61	0.945	1.4303	36.7	3.86	7.96
10	Decalin	C10H18	138.25	196	-43	0.9	1.481	2.2	0	33.8
11	O-Xylene	C8H10	106.17	144.4	-25.2	0,88	1.5055	2.57	0.62	7.56
12	1,2-Dichlorobenzene	C6H4Cl2	147.01	180.5	-17	1.305	1.5515	9.93	2.5	
13	Benzene	C6H6	78.12	80.1	5.5	0.879	1.5011	2.28	0	6.03
14	Toluene	CH3-C6H5	92.15	110.6	-95	0.867	1.4961	2.38	0.36	5.52
15	Chloroform	CHCl3	119.38	61.7	-63.5	1.48	1.4459	4.7	1.87	5.42
16	Ethyl acetate	CH3CO2C2H5	88.12	77.1	-83.6	0.9	1.3723	6.02	1.78	4.41
17	Water	H2O	18	100	0	0.998	1.33299	78.5	1.84	10.1
18	Acetyl Acetone	CH3COCH2COH3								
19	Pyridine	C5H5N	79.1	115.6	-41.8	0.982	1.5095	12.3	2.19	9.45
20	Dimethyl Sulfoxide	(CH3)2SO	78.1	189	-32	1.328	1.3874	42.6		
21	Cyclohexane	C6H12	84.16	80.7	6.55	0.778	1.4266	2.02	0	8.98
22	Phenolphthalein (alcoh.0.5%)									
23	Acetonitril	CH3CN	41.05	81	-44	0.786	1.3441	36.2	3.92	3.45
24	Phenolphthalein									
25	Phenol	C6H5OH	94.11	181.8	43	1.072	1.5418	9.78	1.45	34.9
26	Dimethyl Sulfate	(CH3O)2SO2	126.13	188	-32	1.333	1.3874	42.6		

Table 4. Properties of organic solvents. (Concluded)

##	Name (abbrev.)	Formula	Mol.Wt.	B.p. C	M.p.C	density,	diel.const	refraction	b.moment	viscosity
27	Decane	C10H22	142.29	174	-30	0.73	1.4102	1.99	0	8.54
28	Cyclodecane	C10H20	140	201		0.871				
29	Cycloheptane	C7H14	98.12	118.5	-12	0.811	1.4436			
30	Cycloheptene	C7H12	96.17	112		0.824				
31	2.2-Pyridil									
32	Pyridazine	C4H4N2	80.09	208		1.103				
33	Piperazine	C4H4(NH)2	86.14	145						
34	Piperidine	C5H11N	85.15	106	-10.5	0.861	1.453	5.8	1.2	
35	Perfluorohexane	CF3(CF2)4CF3	338	59	-4	1.669				
36	Trifluorotoluene	CF3-C6H5	146.1	103	-29	1.189				
37	Pentane	CH3(CH2)3CH3	72.2	36	-130	0.626	1.3575	1.84	0	2.15
38	Carbon tetrachloride	CCl4	153.8	77	-23	1.584	1.4601	2.23	0	9.69
39	Tetrahydrofuran (THF)	C4H8O	72.1	66	-109	0.889	1.405	7.32	1.63	
40	Ethylene glycol	HOCH2CHOH	62.1	197	-13	1.114				
41	Glycerol		46	290	18	1.261	1.4735	42.5	2.56	9450

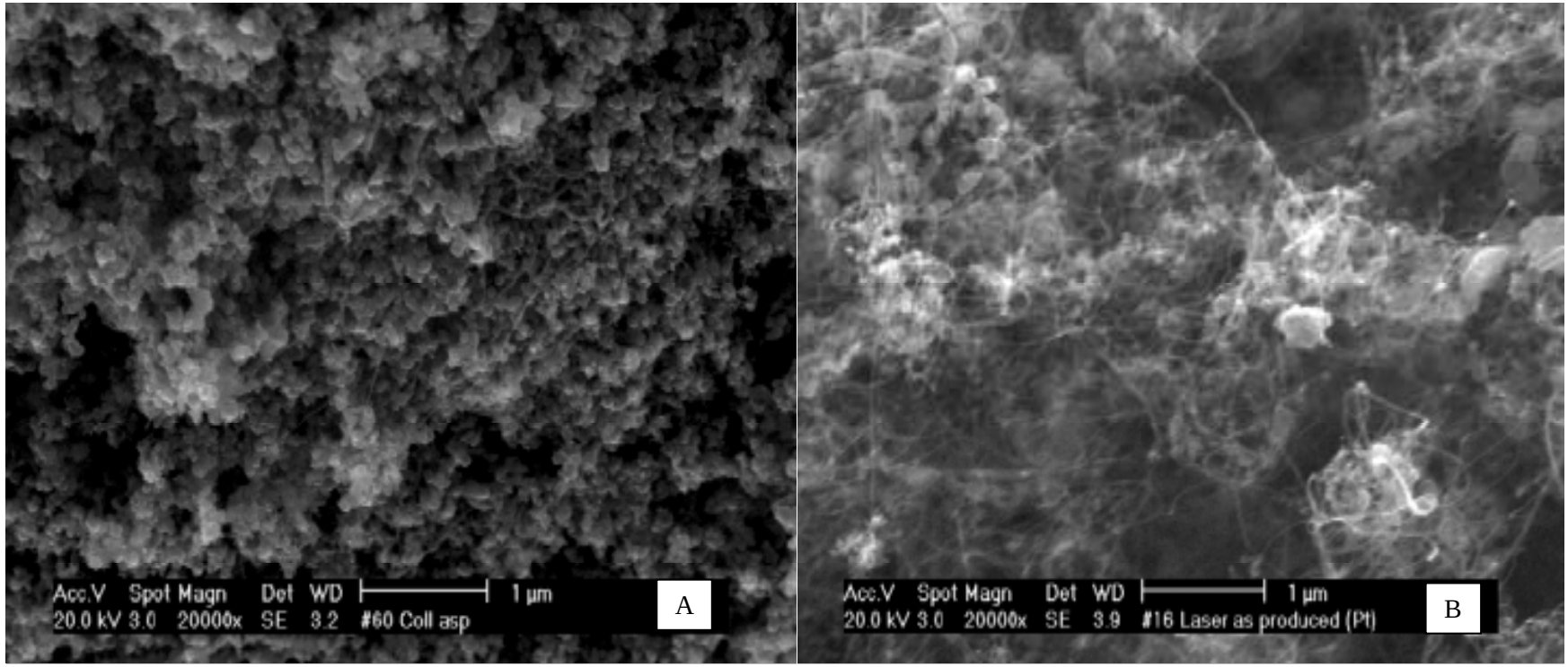

Figure 1. As-produced material
A. Arc produced material (as-made) (collarette #60). B. Laser produced material (as-made) (run#16).

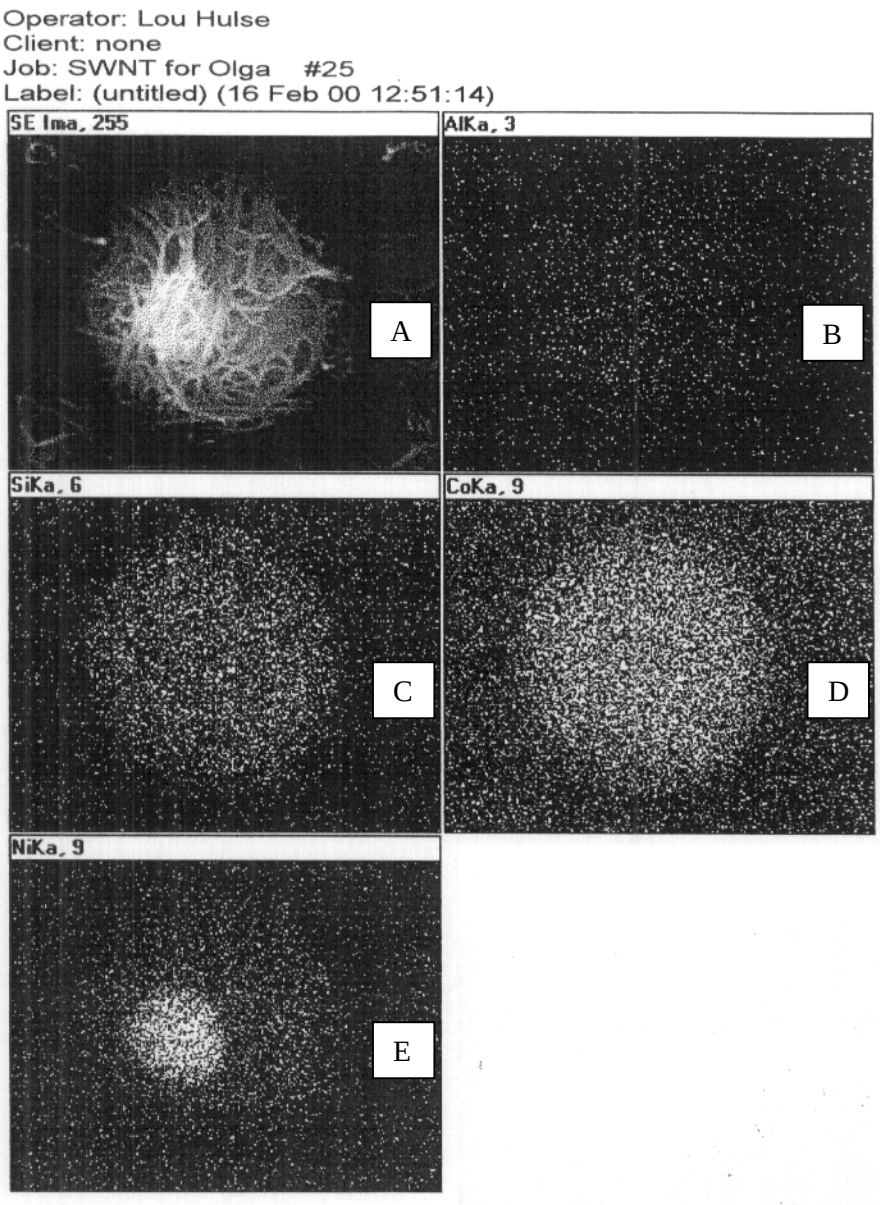

Figure 2. Elemental maps of encapsulated catalyst particle. A. Secondary electron SEM image. B. Aluminum. C. Silicon. D. Cobalt. E. Nickel.

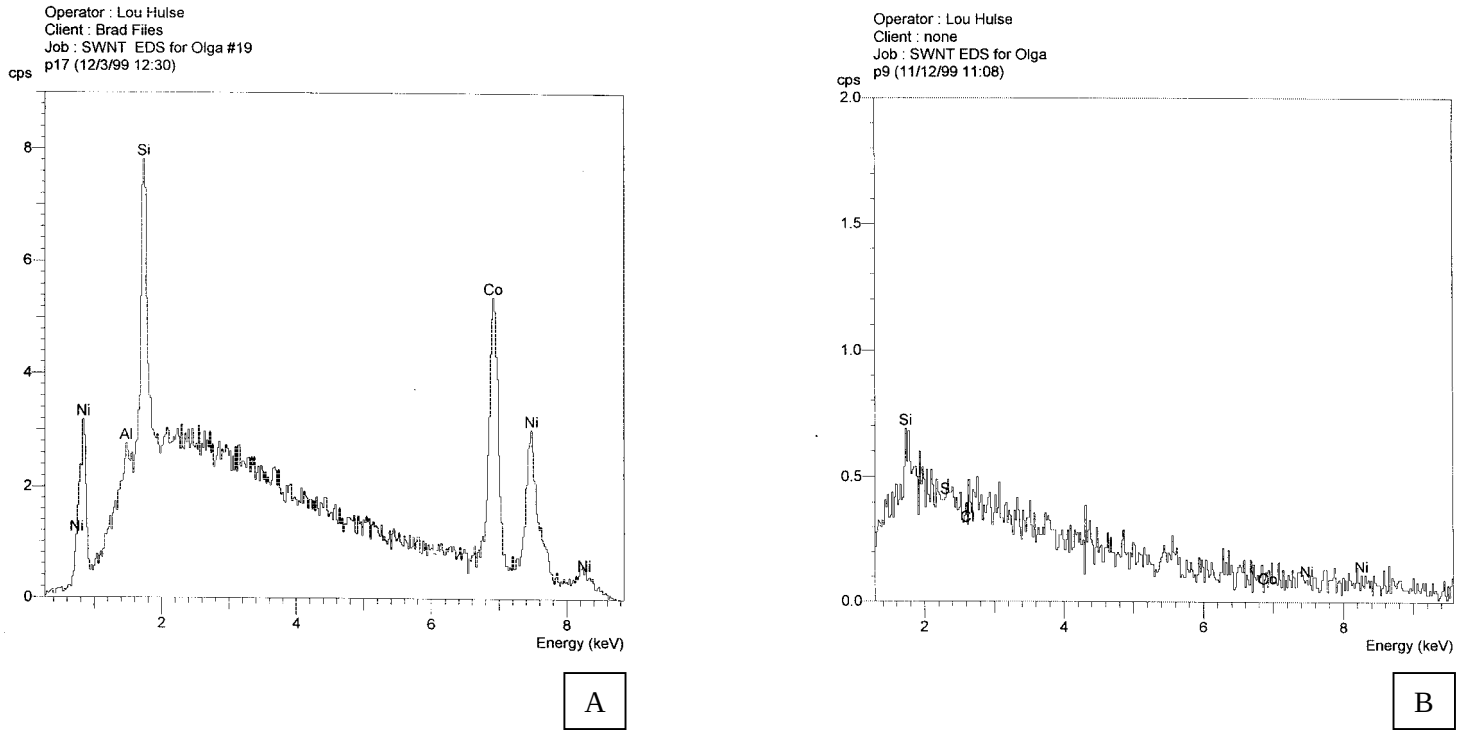

Figure 3. EDS characterization of laser-made sample (#10). This is spectra averaged over approximately 20x30 μm area on the SEM specimen. A. Before purification. B. After purification.

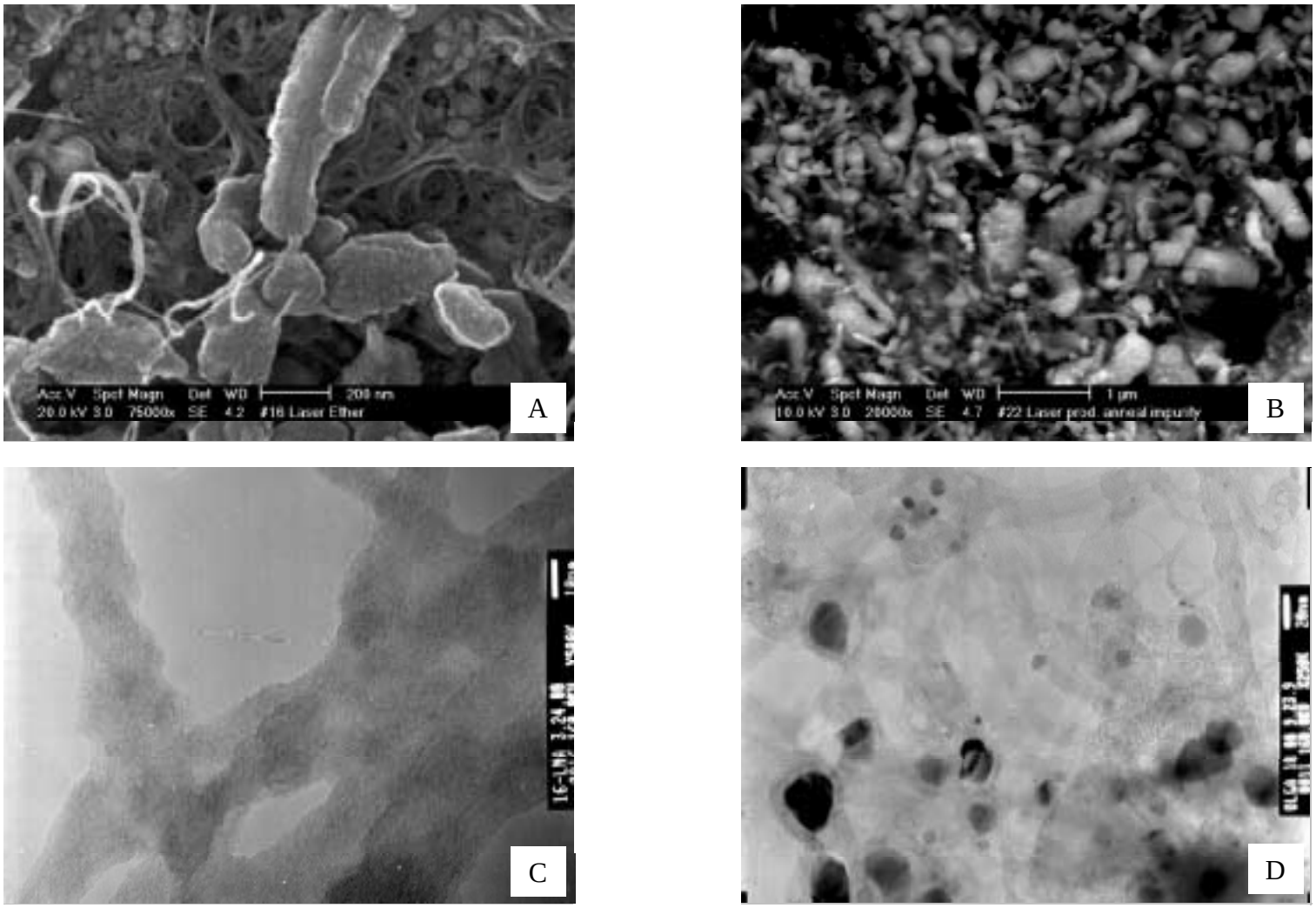

Figure 4. Impurities in laser-made samples. A. Laser sample (#16) washed by ether (SEM). B. Laser sample (#22) after annealing, ash-like residue (SEM). C. Laser sample (#16), decant after centrifugation in water-acid suspension (TEM). D. Laser sample (#18) before purification.

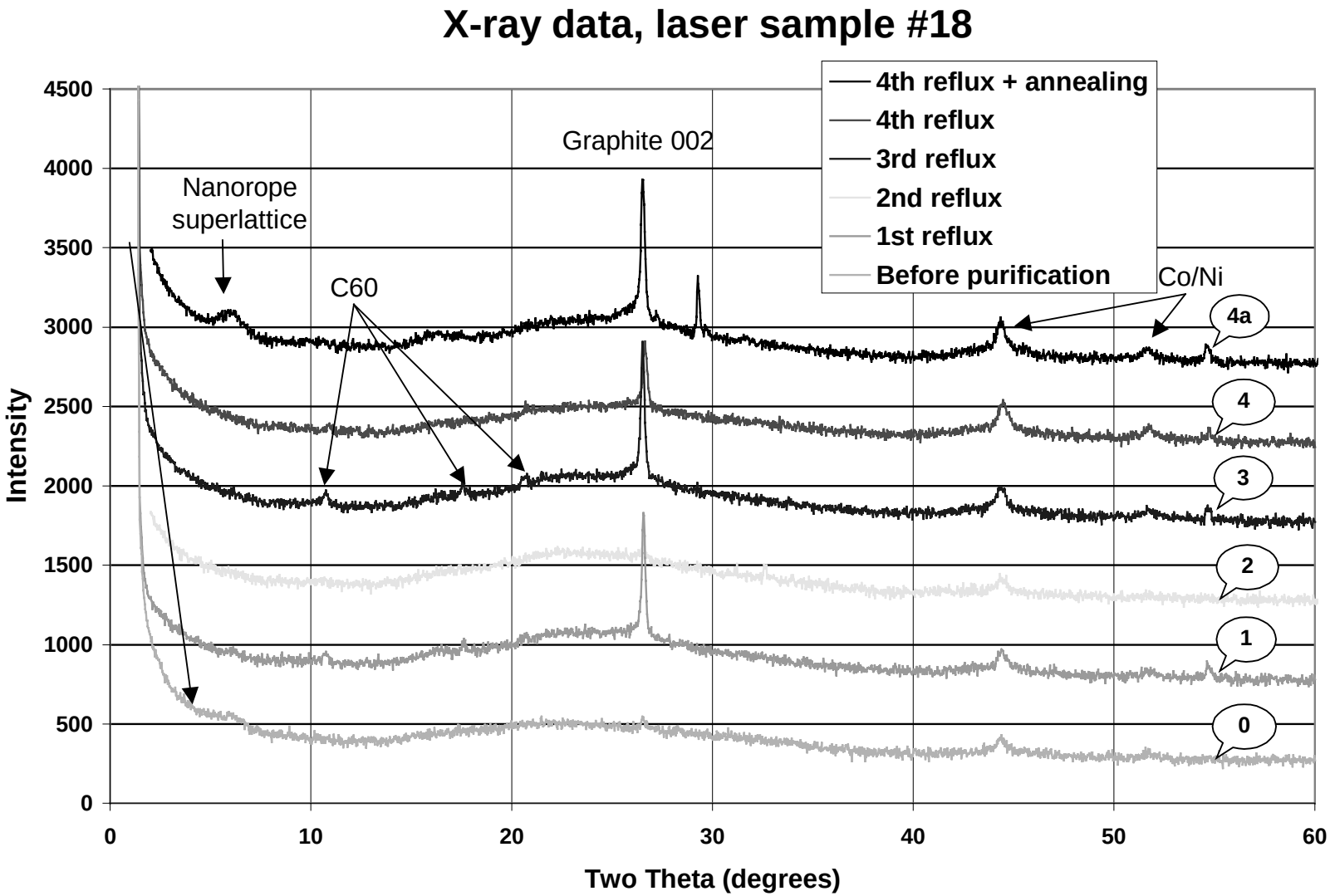

Figure 5a. X-ray diffraction characterisation of laser sample #18 after consequent refluxes

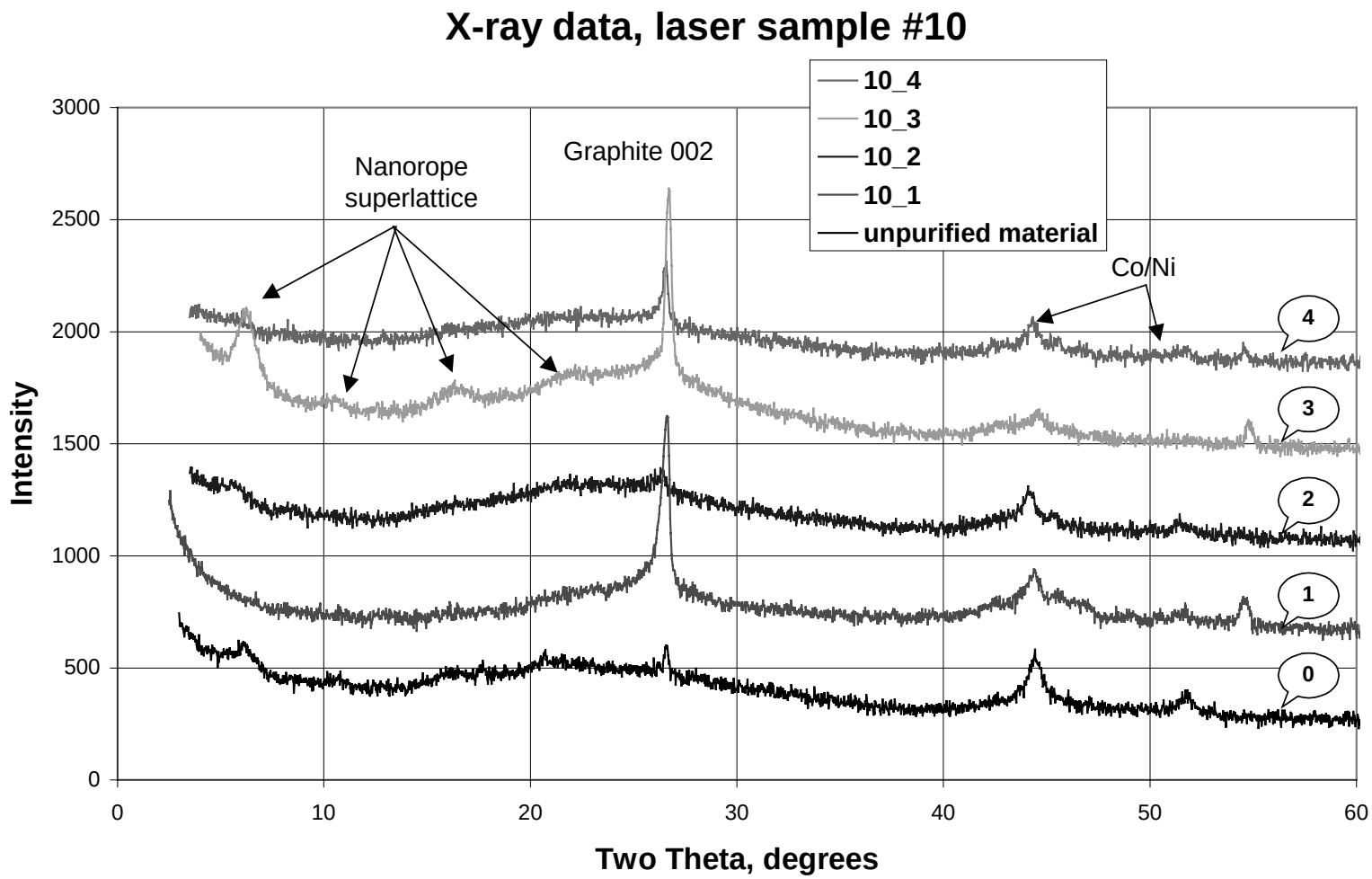

Figure 5b. X-ray diffraction characterisation of laser sample #10 after purification by various techniques.

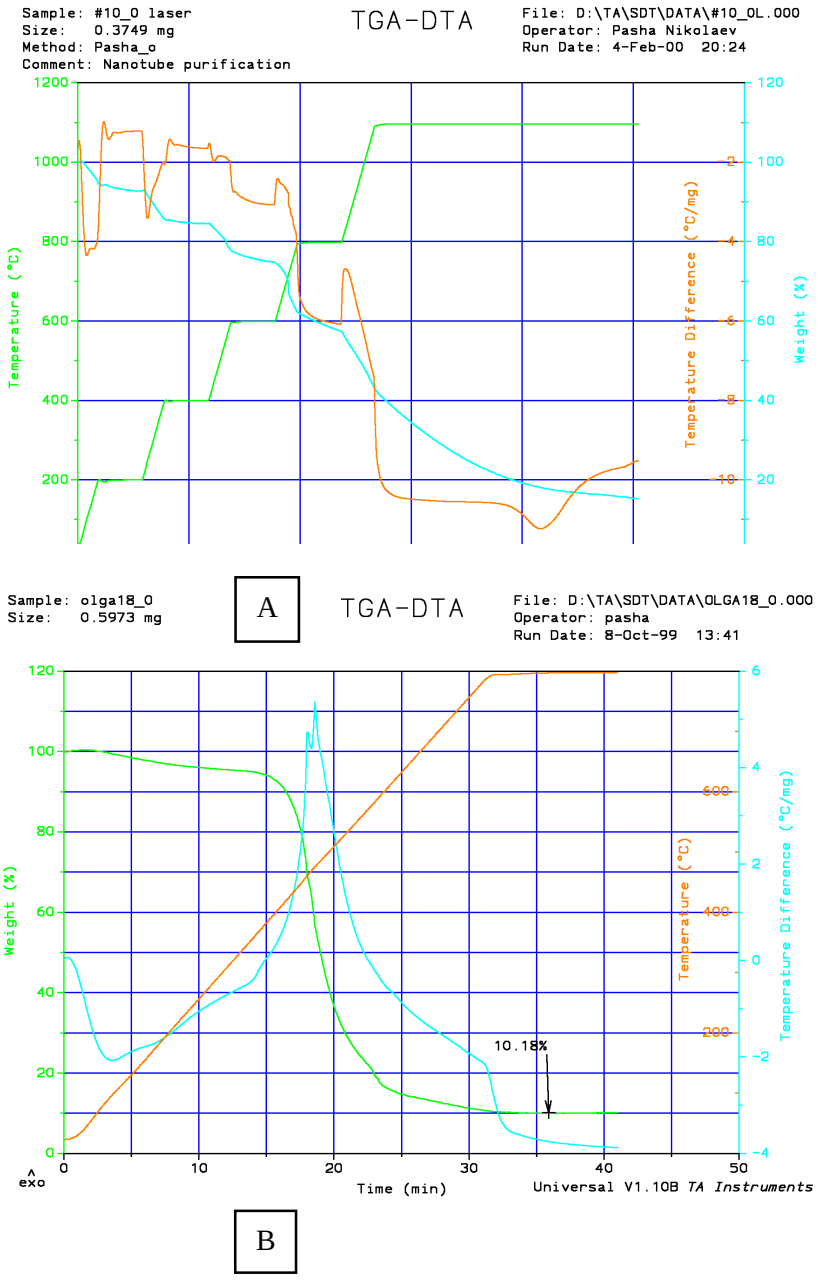

Figure 6. TGA data on unpurified samples. Samples were sublimed in argon flow at 5°C/min up to 800°C.
A. Laser sample #10. Mass left is approximately 18%. Temperature is increased in 200 °C steps.
B. Laser sample #18. Mass left is approximately 10%. Temperature is increased linearly.

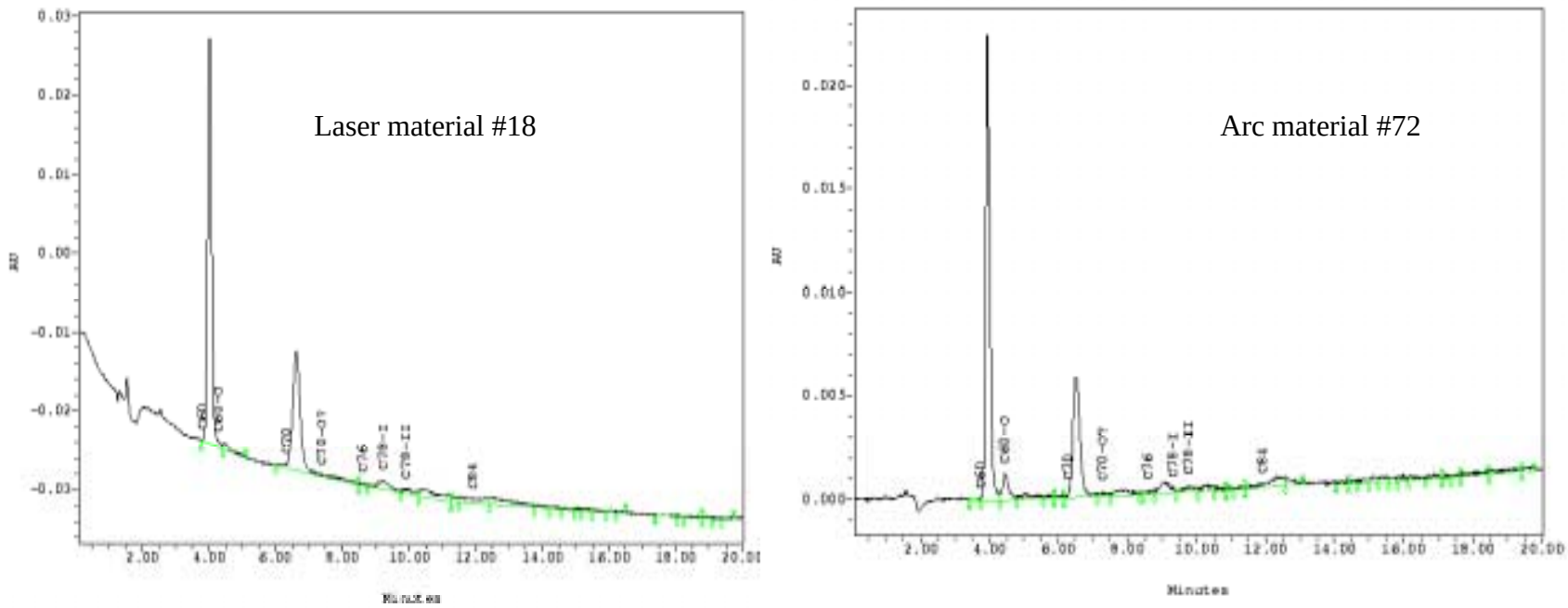

Figure 7. Chromatograms taken on Waters HPLC with Cosmosil column and PDA detector at 304 nm wavelength, mobile phase 2ml/min of toluene.. Laser oven produced nanotubes as well as arc discharge produced nanotubes typically contain 3-5 % of soluble fullerenes by weight, mostly C_{60} and C_{70} in 5:2 ratio.

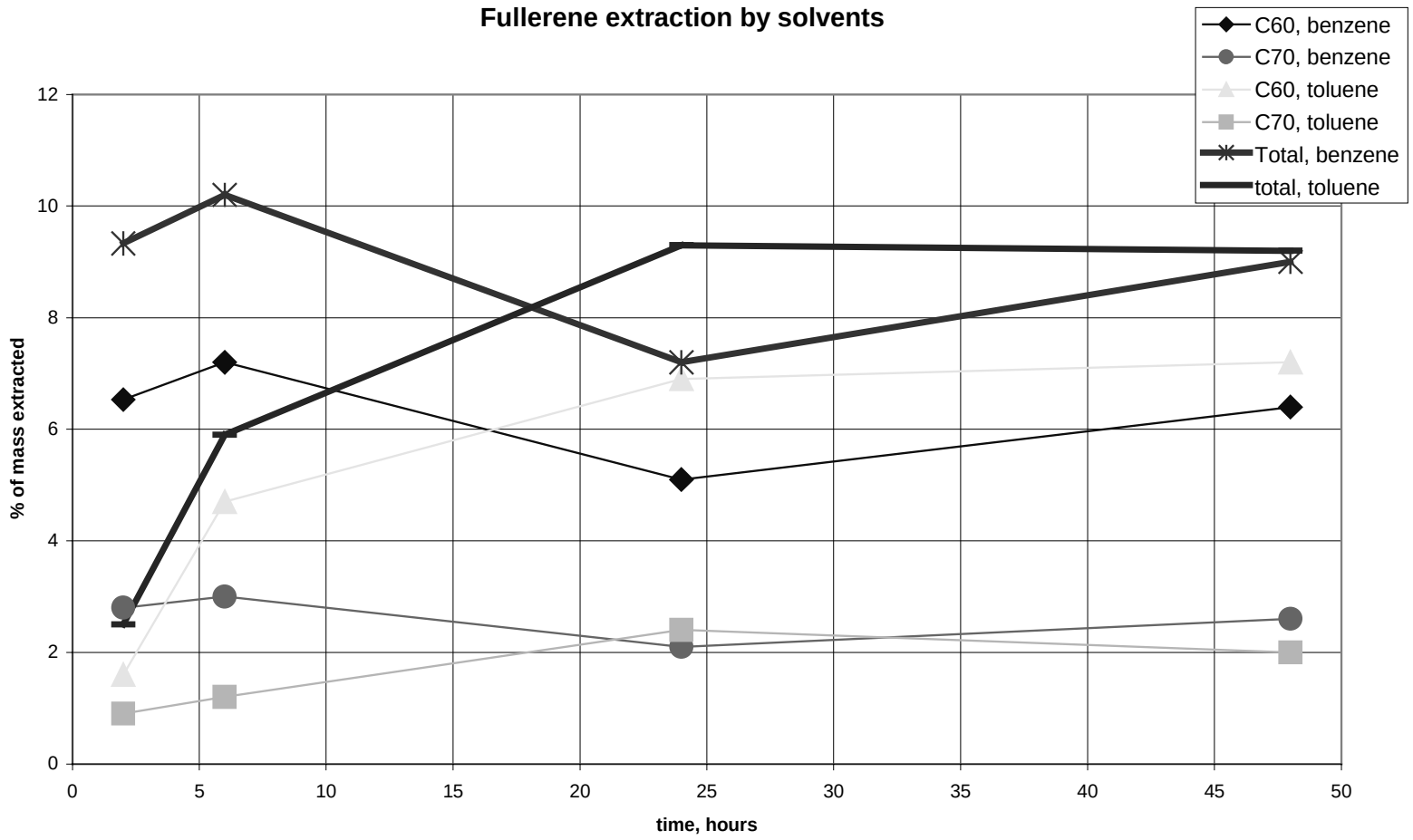

Figure 8. Fullerene extraction by toluene and benzene.

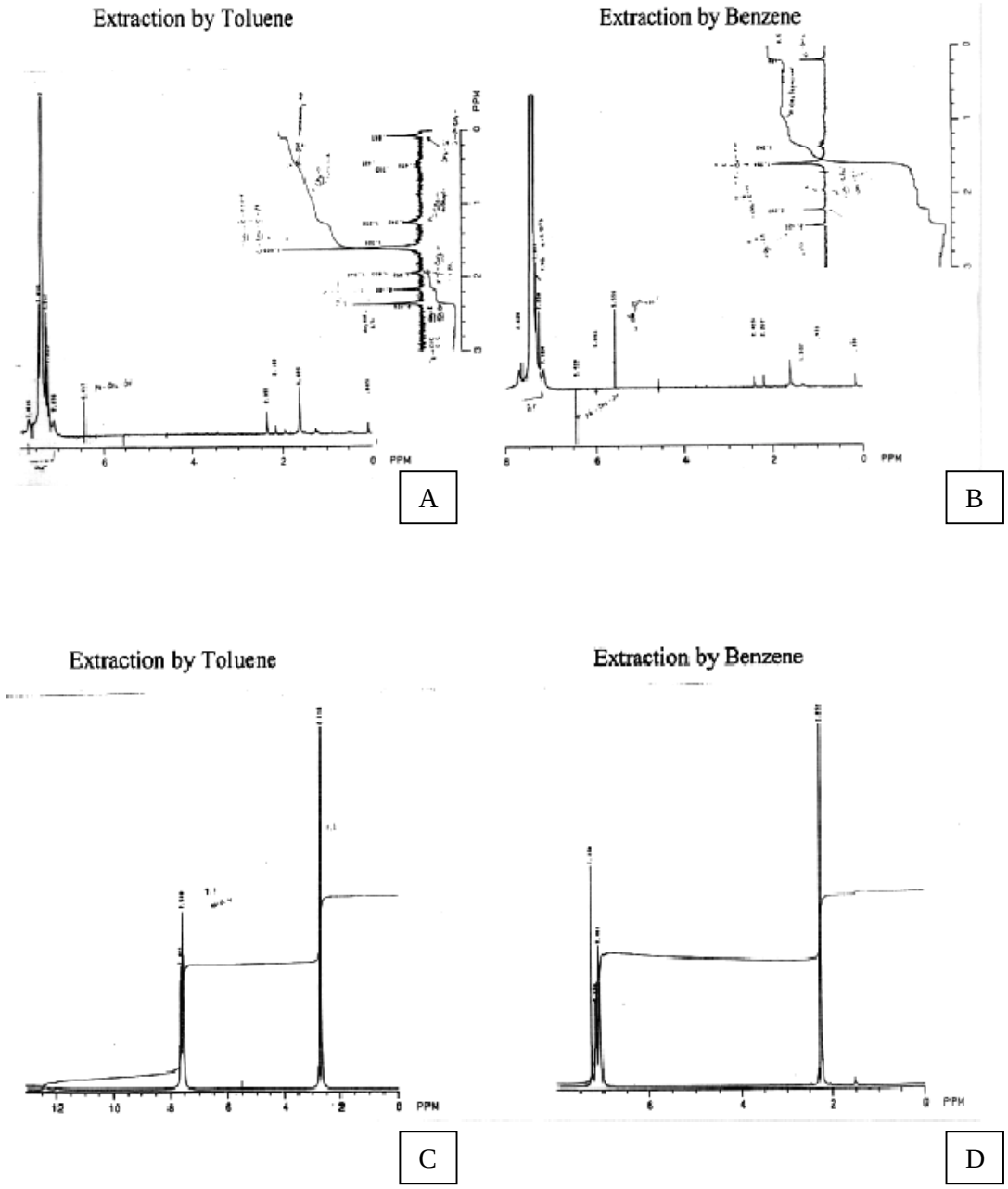

Figure 9. NMR spectra of solvent extracts of as-made nanotube samples.

A. Laser sample #18 extracted by toluene for 8 hrs.
B. Laser sample #18 extracted by benzene for 8 hrs.
C. Arc sample #72 (collarette) extracted by toluene for 8 hrs.
D. Arc sample #72 (collarette) extracted by benzene for 8 hrs.

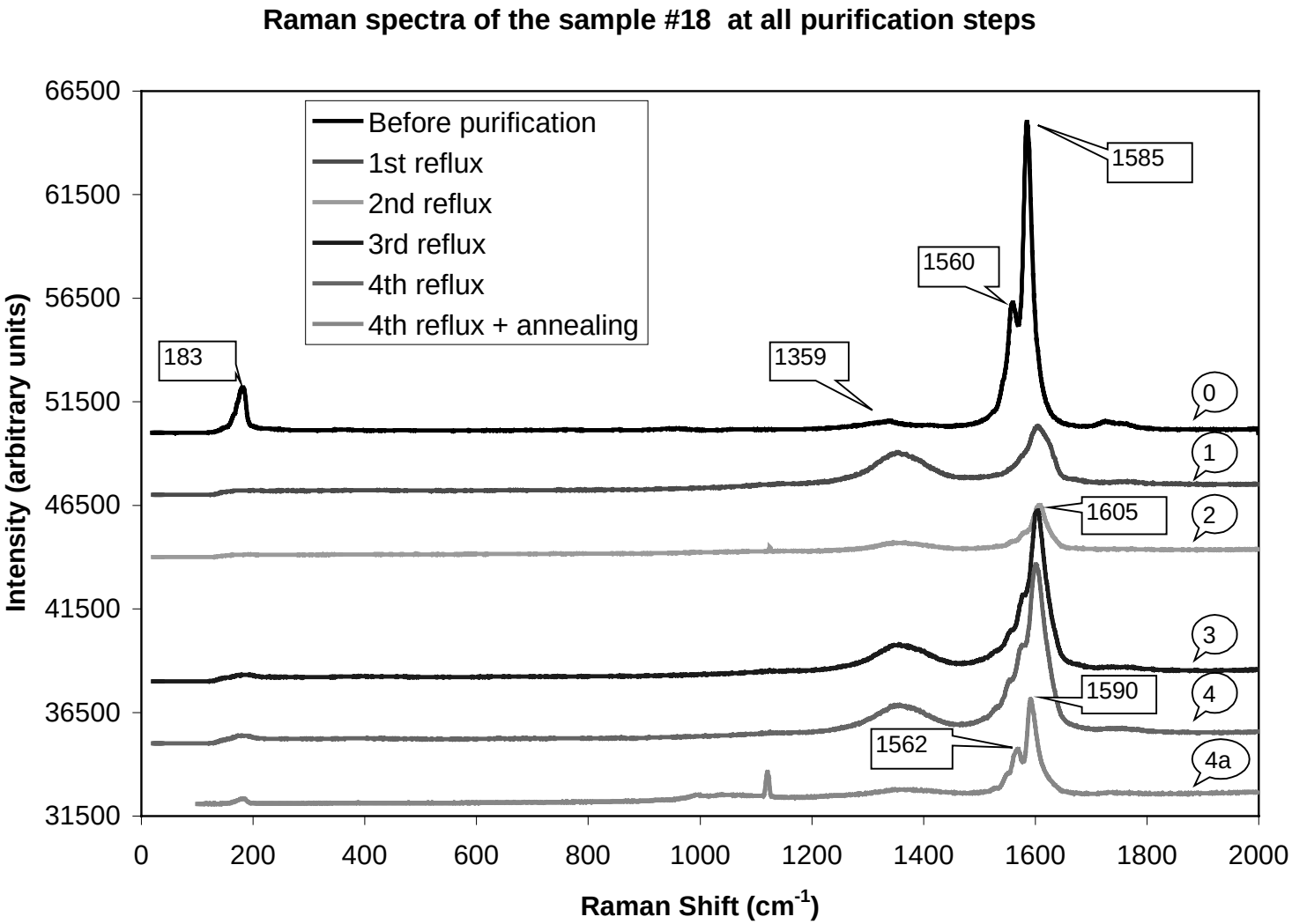

Figure 10a. Raman spectra of laser sample #18 after consequent refluxes

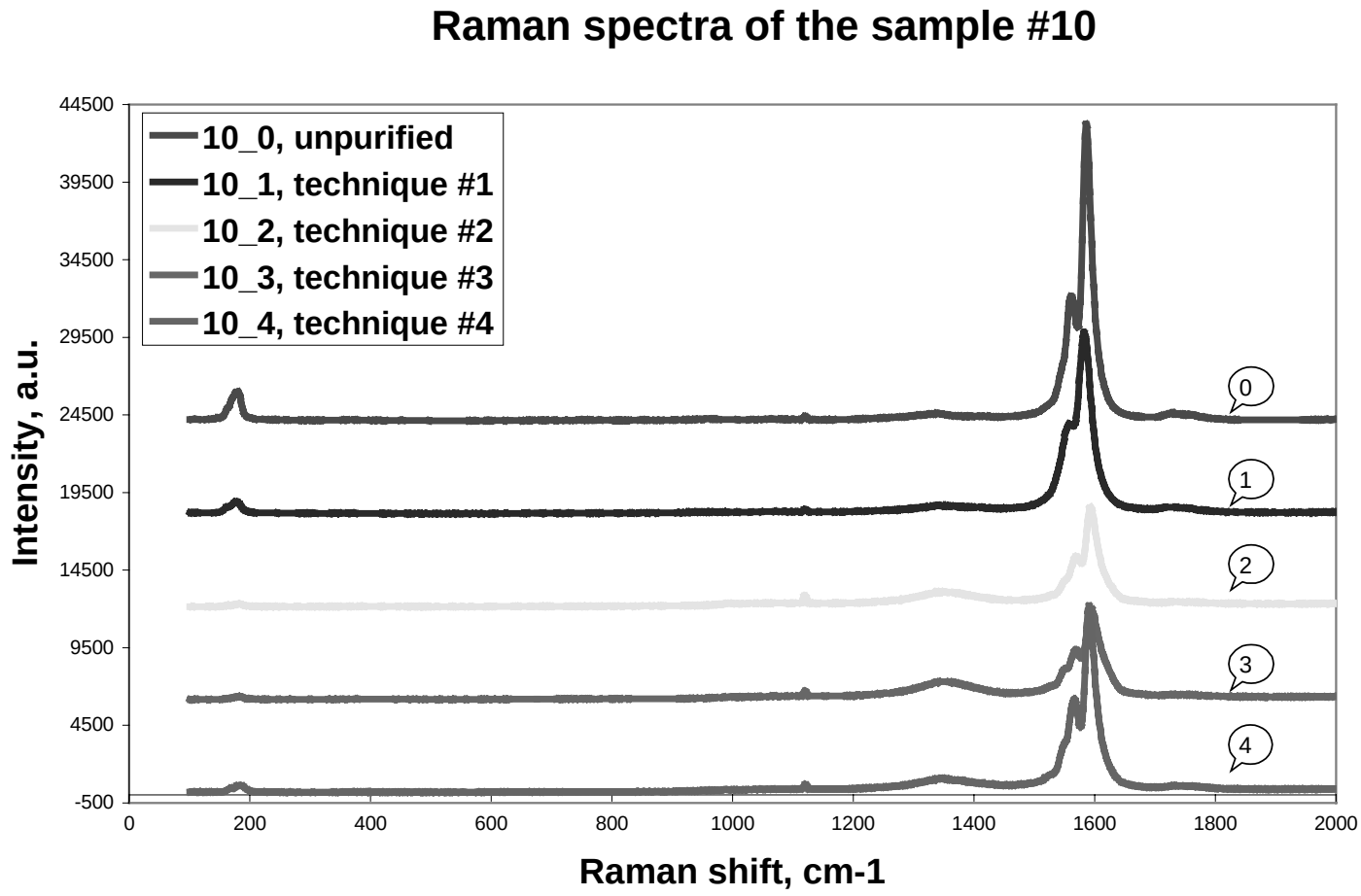

Figure 10b. Raman sectra of laser sample #10 after purification by various techniques.

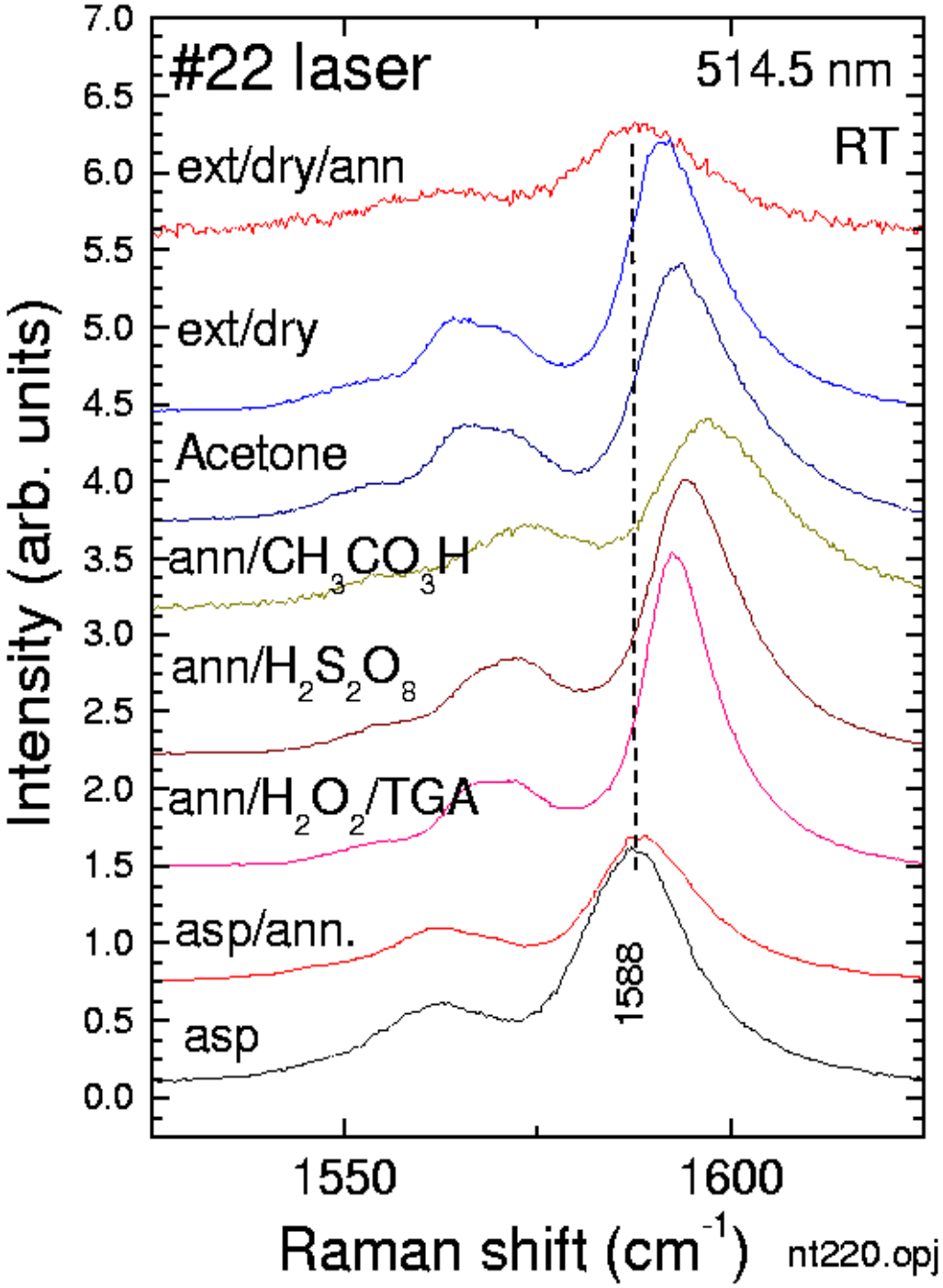

Figure 11. Raman spectra of laser sample #22 purified by various techniques and suspended in various organic solvents.

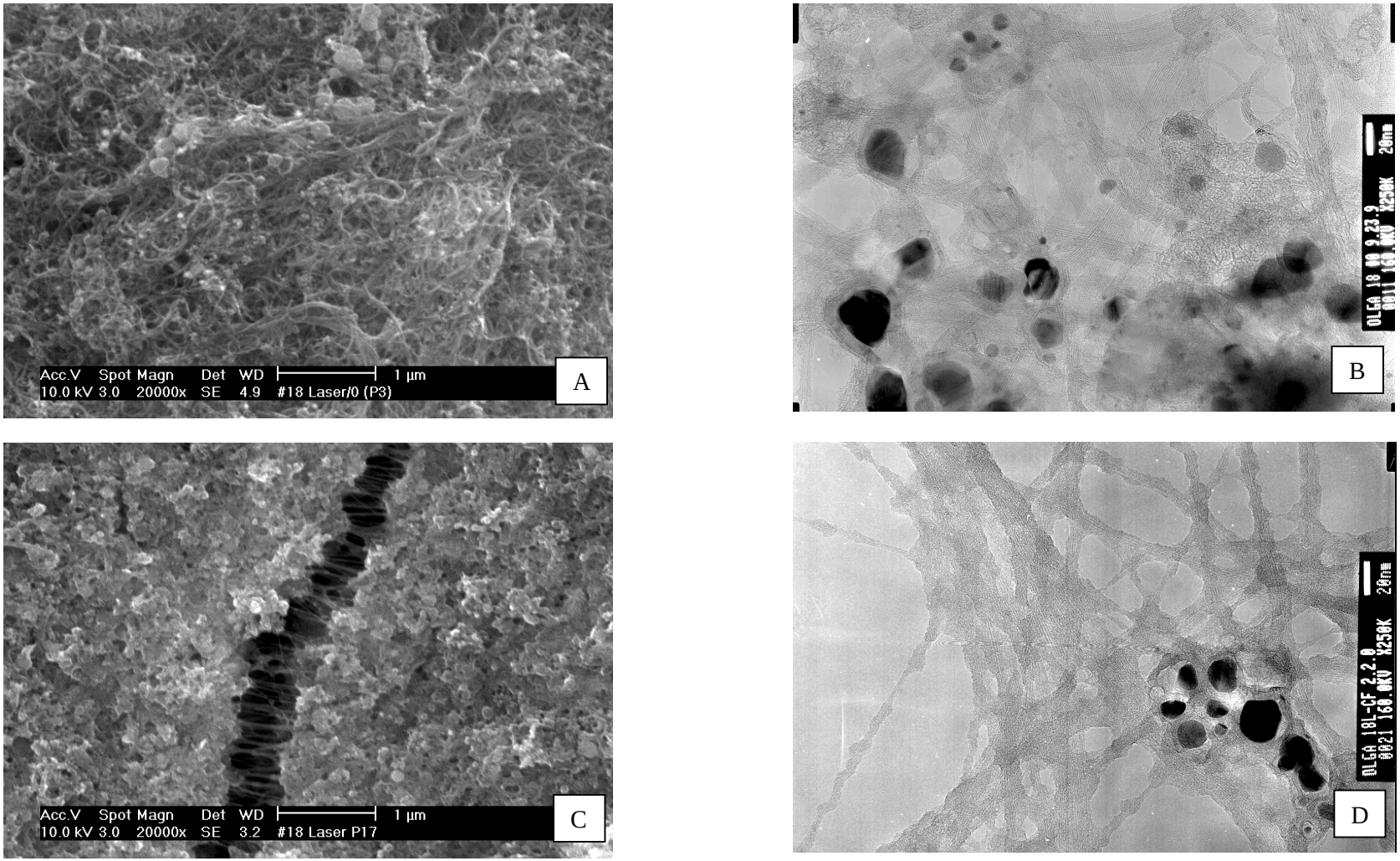

Figure 12. Laser sample #18 before (A,B) and after (C,D) purification by "Old Rice method" using cross-flow filtration. Amorphous coating on nanotubes essentially did not change.

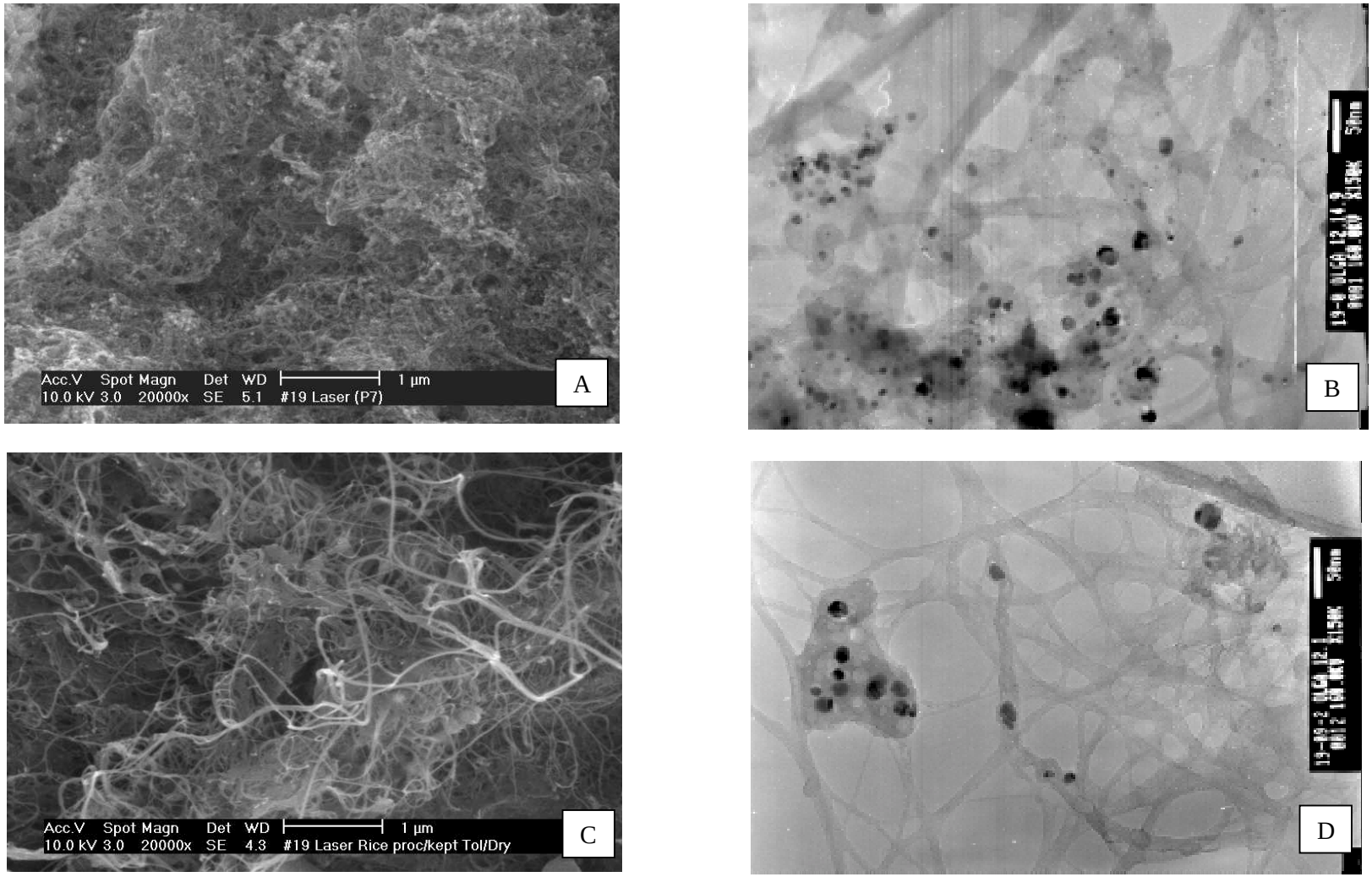

Figure 13. Laser sample #19 before (A,B) and after (C,D) purification by "New Rice method".

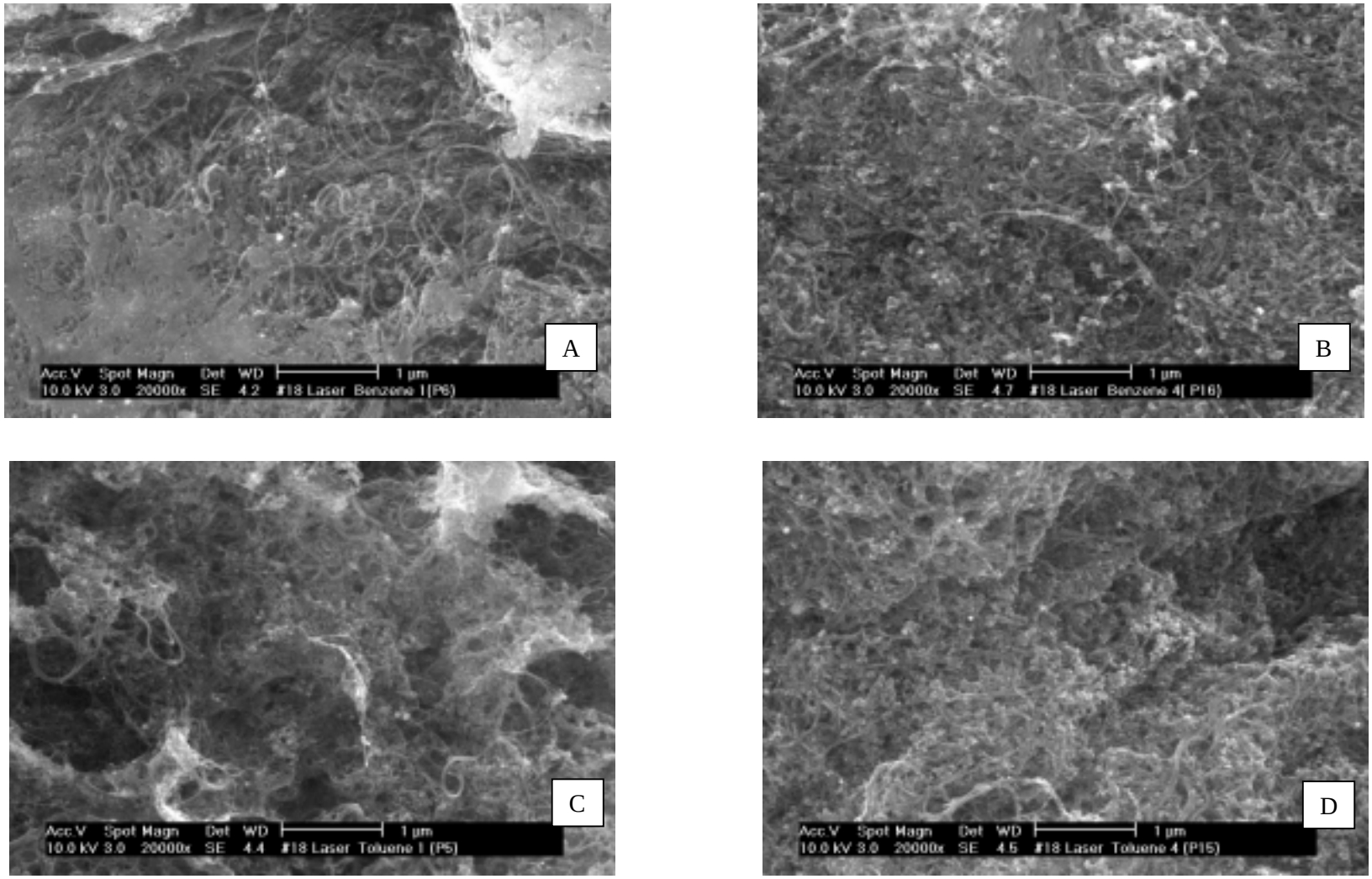

Figure 14. Laser sample #18 after solvent extraction.
A. After 3 hrs of benzene extraction. B. After 48 hrs of benzene extraction. C. After 3 hrs of toluene extraction. D. After 48 hrs of toluene extraction.

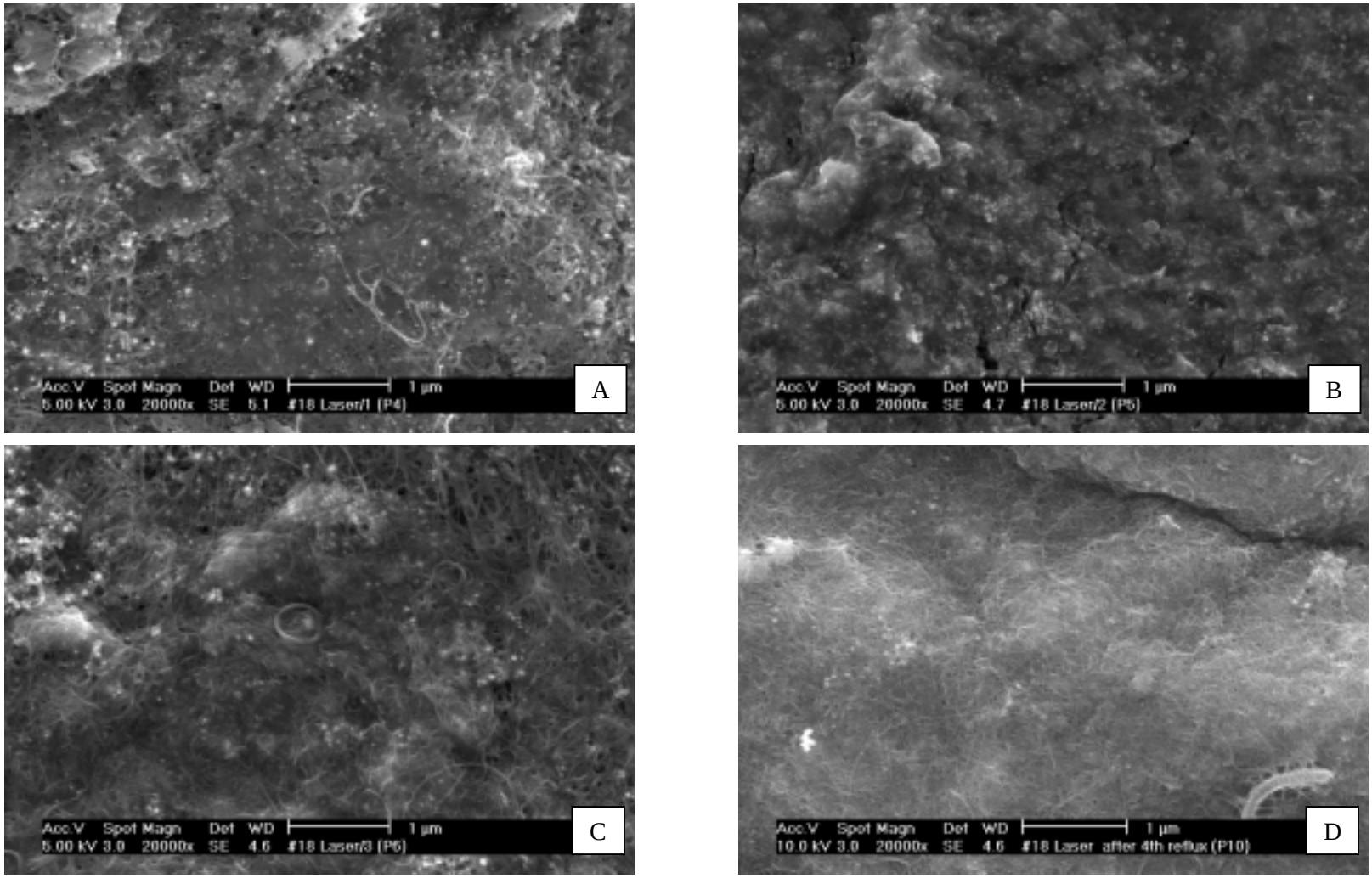

Figure 15. Sample #18 after consequent refluxes in HNO_3. A. 1st reflux. B. 2nd reflux. C. 3rd reflux. D. 4th reflux.

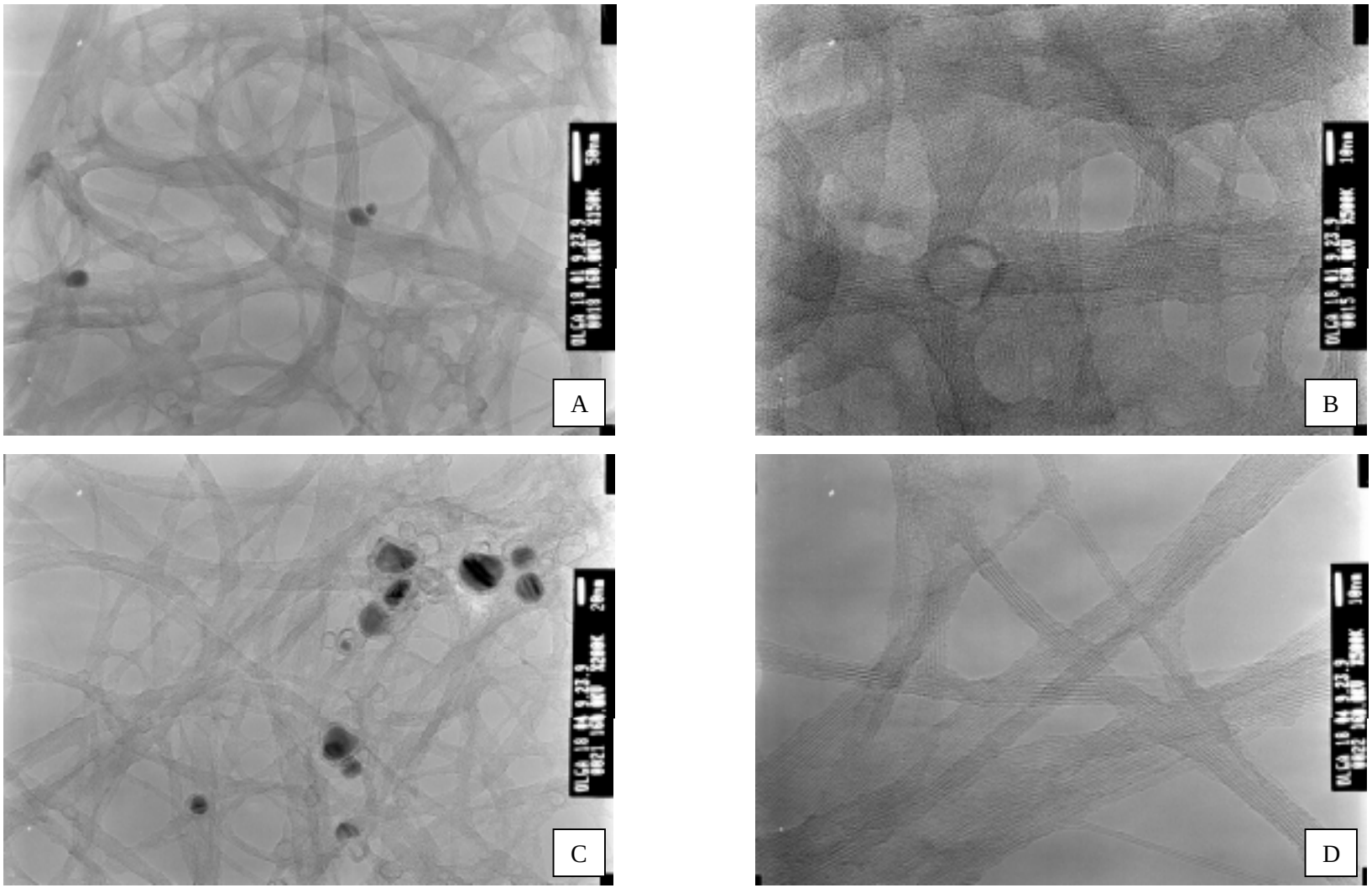

Figure 16. Laser sample #18 after subsequent refluxes in HNO_3. A,B. After first reflux. C,D. After fourth reflux.

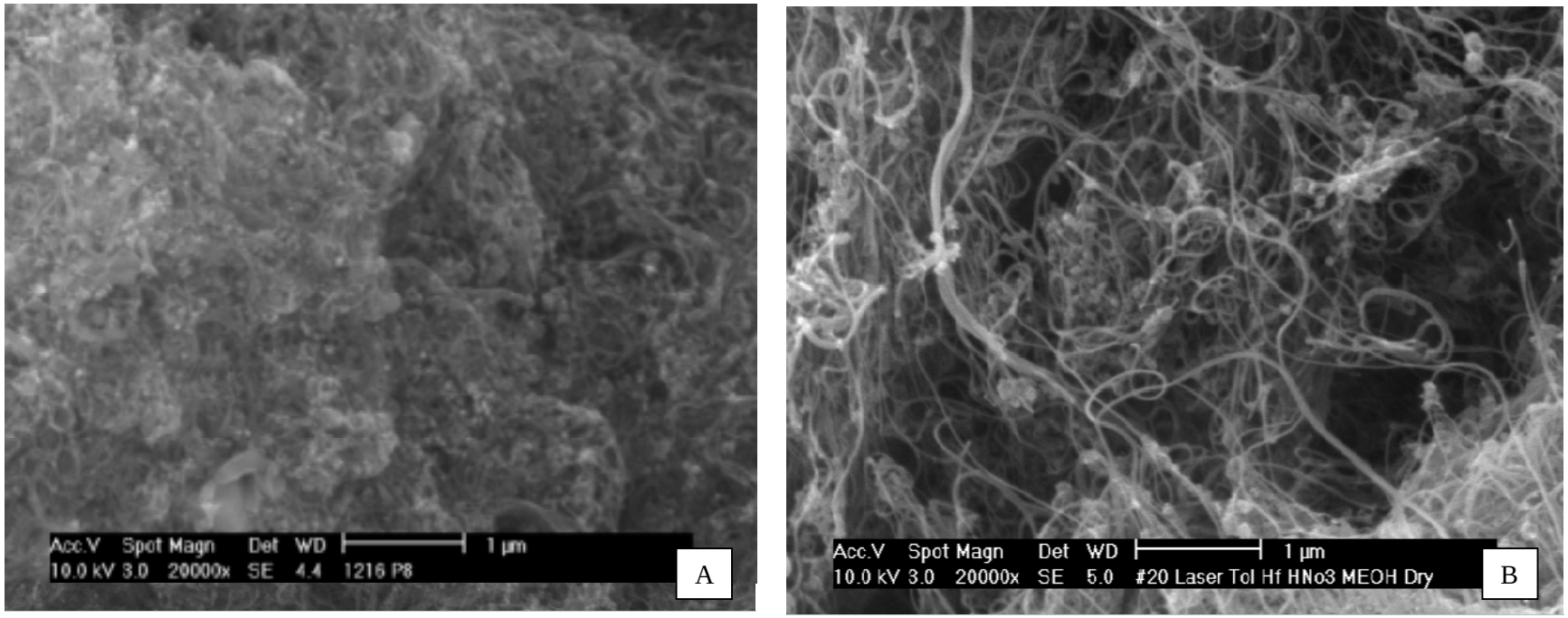

Figure 17. Laser sample #20 purified by toluene extraction followed by reflux in HF with addition of HNO_3, washed by methanol and dryed in the oven at 100°C.
A. Unpurified. B. Purified.

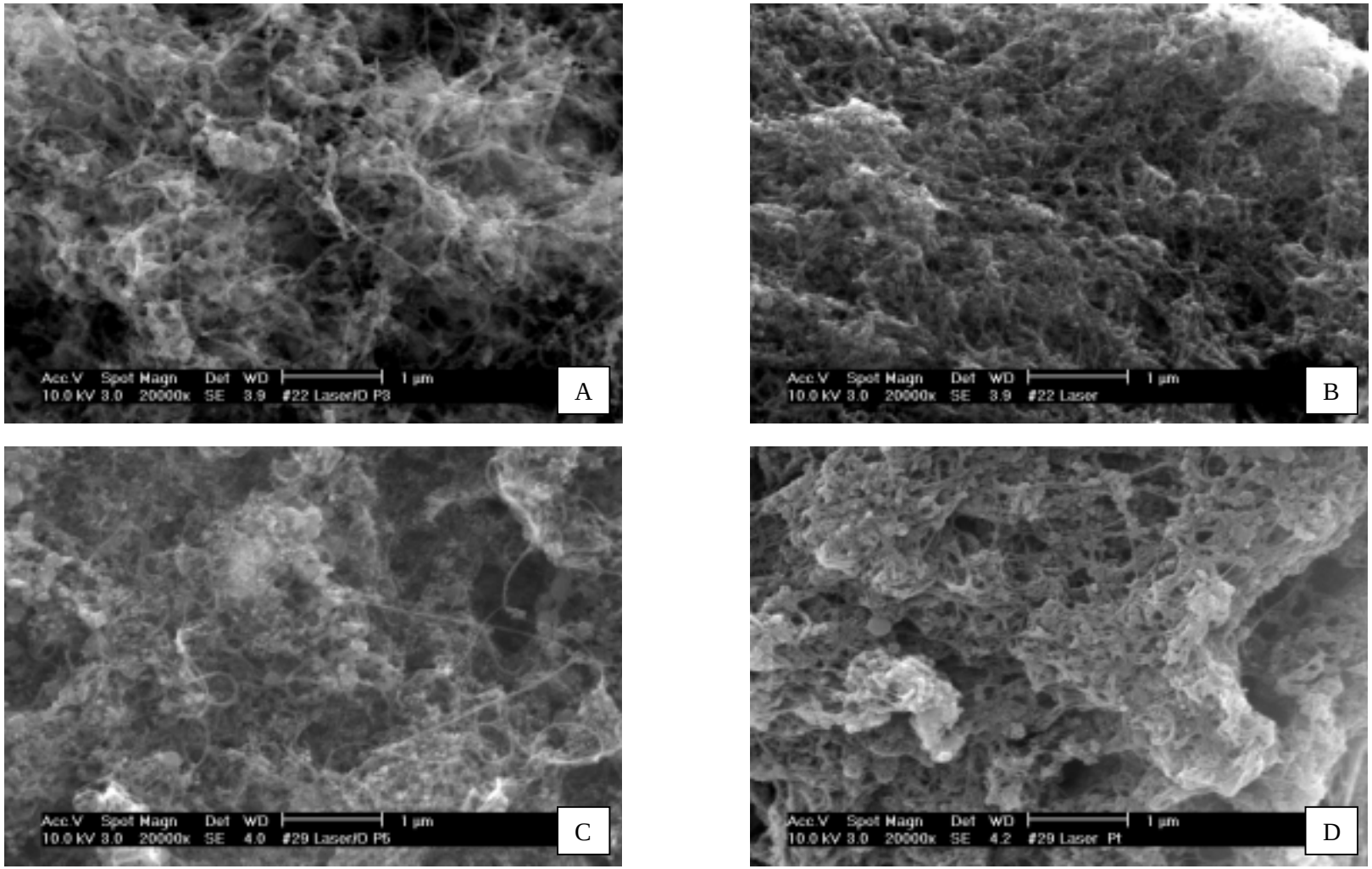

Figure 18. Laser samples #22 and 29 before and after toluene extraction and reflux in HCl.
A. #22 unpurified. B. #22 after purification. C. #29 unpurified. D. #29 after purification.

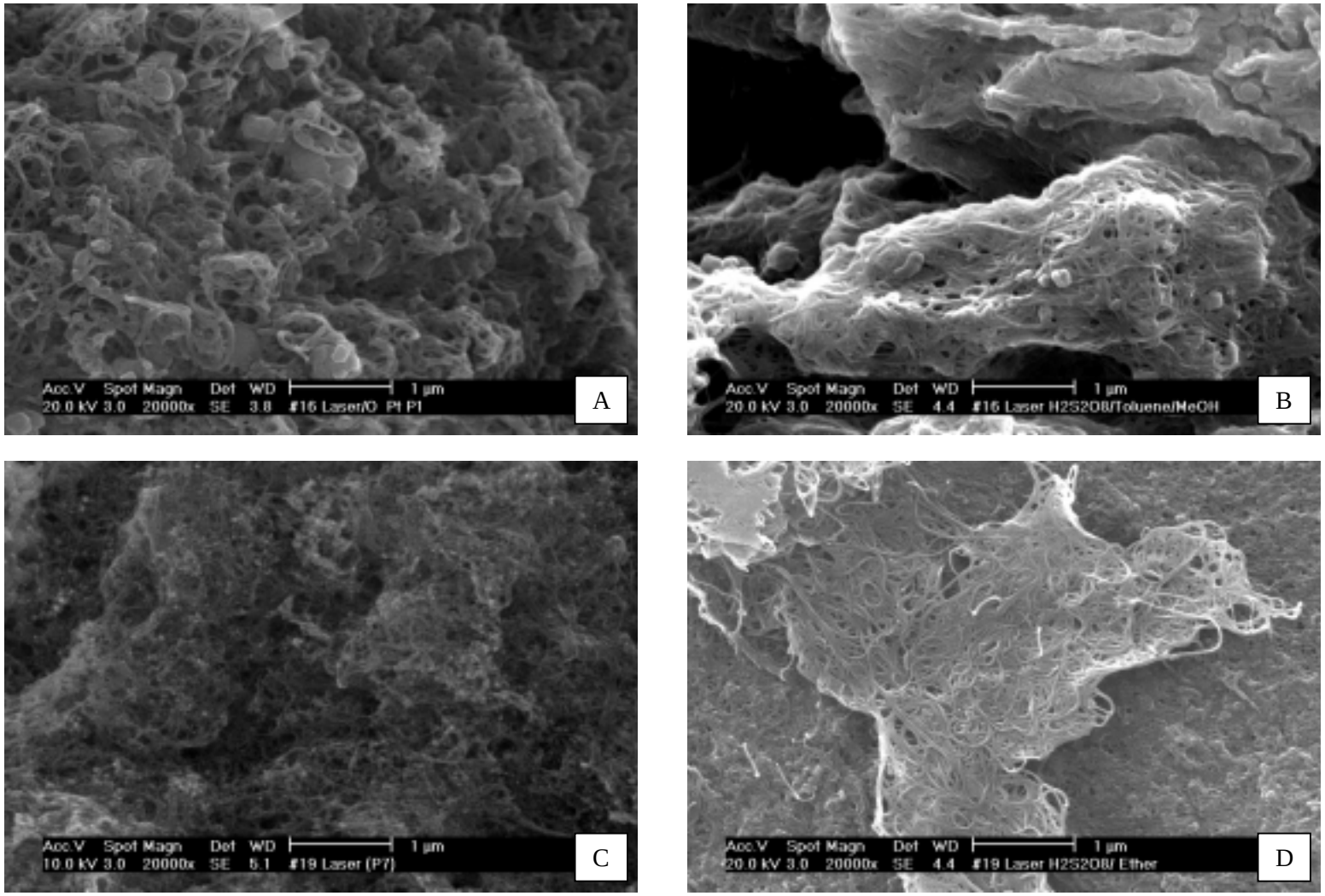

Figure 19. Laser samples #16 and 19 before and after purification by toluene extraction followed by $H_2S_2O_8$.
A. #16 unpurified. B. #16 purified. C. #19 unpurified. D. #19 purified.

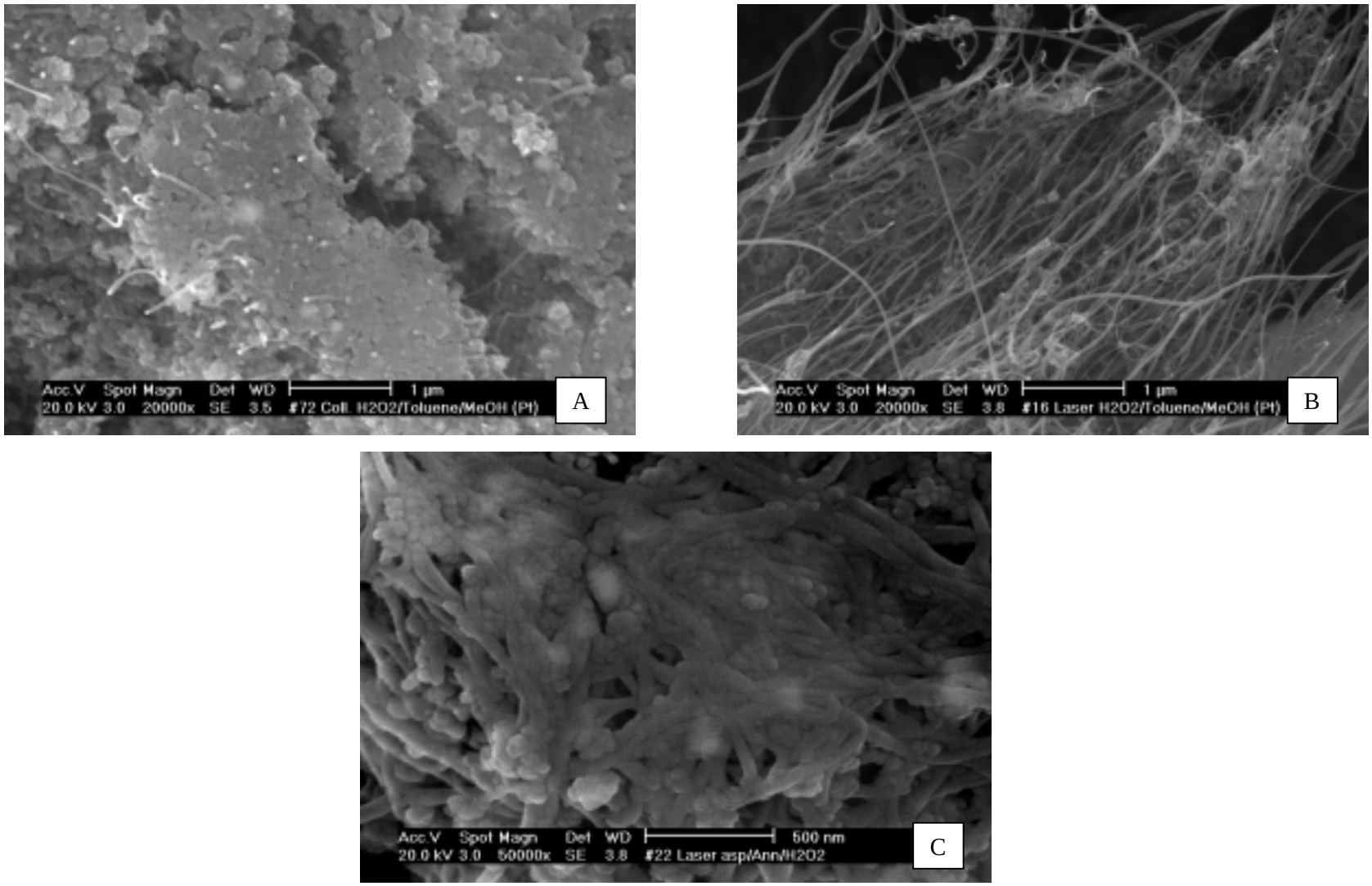

Figure 20. Laser samples #16, 22 and arc sample #72 purified by toluene extraction followed by reflux in H_2O_2
A. Arc sample #72 (collarette). B. Laser sample #16. C. Laser sample #22.

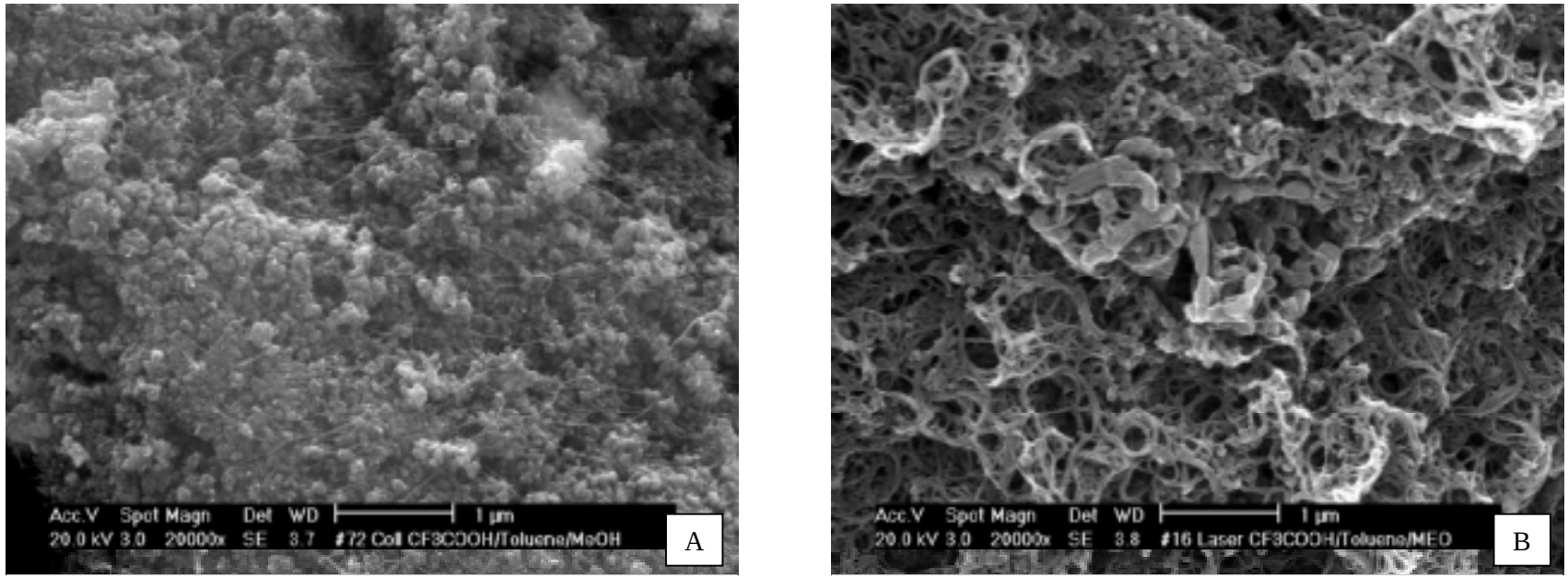

Figure 21. Arc sample #72 (A) and laser sample #16 (B) and purified by toluene extraction followed by oxidation by trifluoroacetic acid (CF_3COOH)

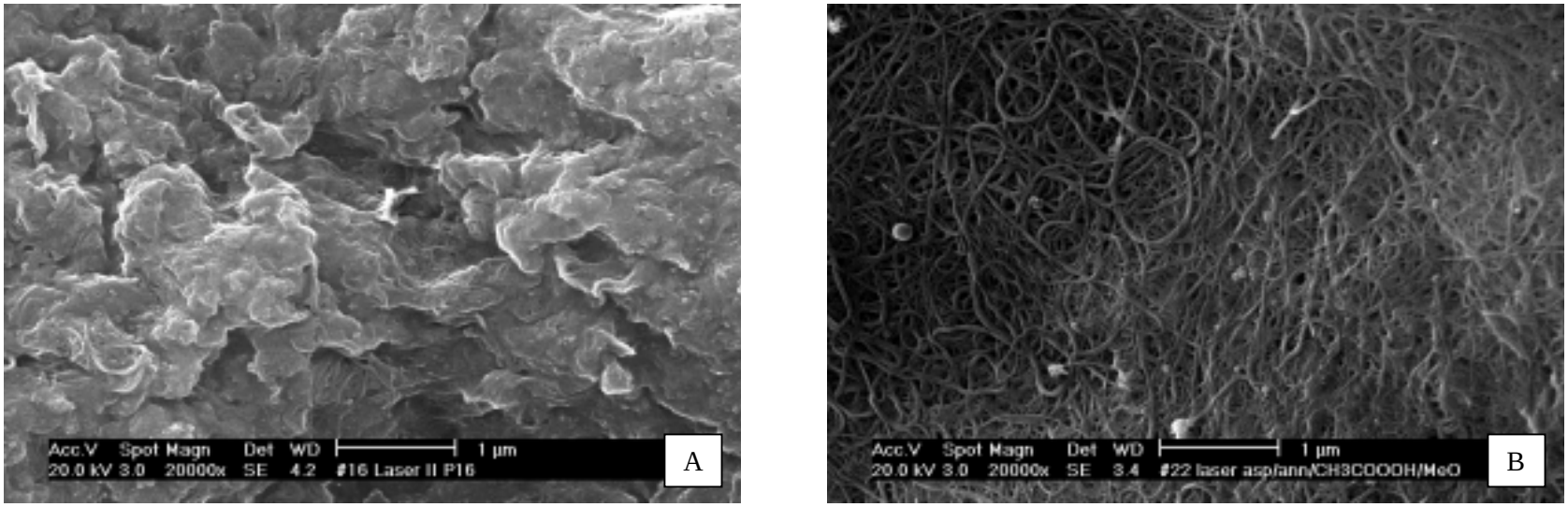

Figure 22. Laser samples #16 and #22 purified by peroxyacetic acid (CH_3COOOH).
A. Toluene extraction followed by reflux in peroxyacetic acid. B. Vacuum annealing followed by reflux in peroxyacetic acid.

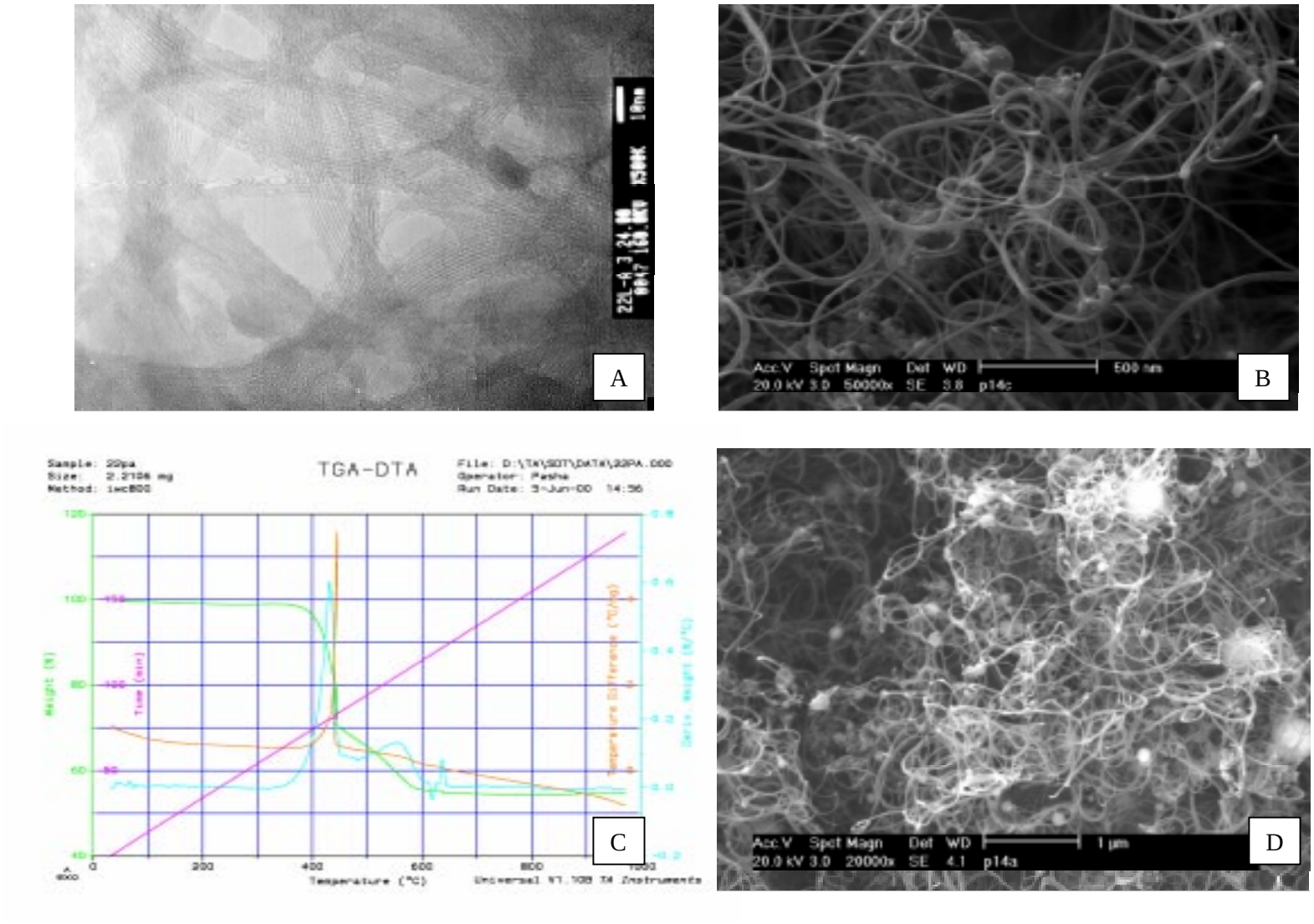

Figure 23. Laser sample #22 purified by vacuum annealing at 1000°C. A. TEM after annealing. B,D. SEM after annealing. C. TGA data in air flow after annealing. There's approx. 54 % of mass left after burning at 800°C.

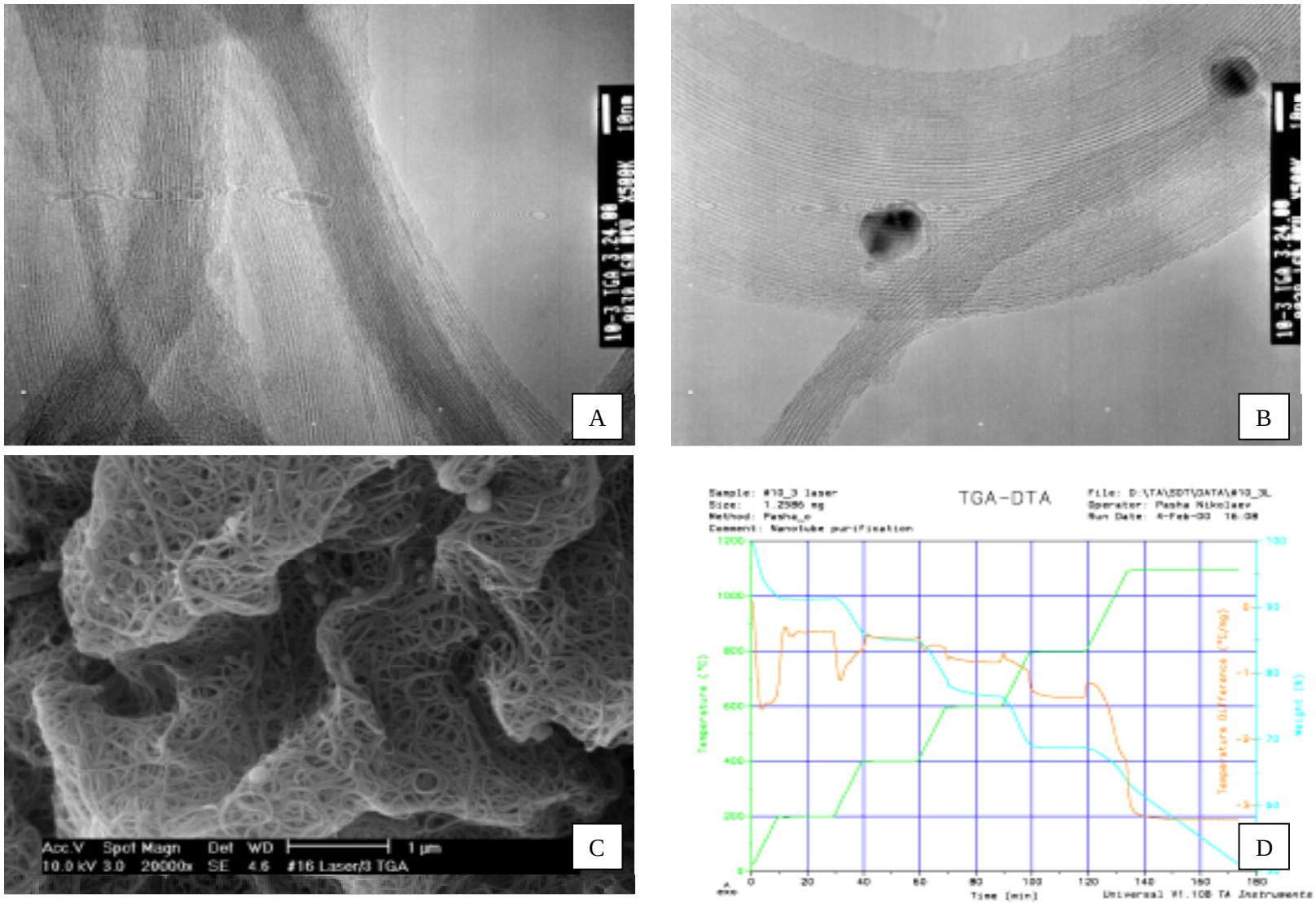

Figure 24. Laser sample #10, purified by toluene extraction followed by reflux in HNO_3 and annealing in argon flow at 1100°C. A,B - TEM images. C - SEM image. d - TGA data during annealing.

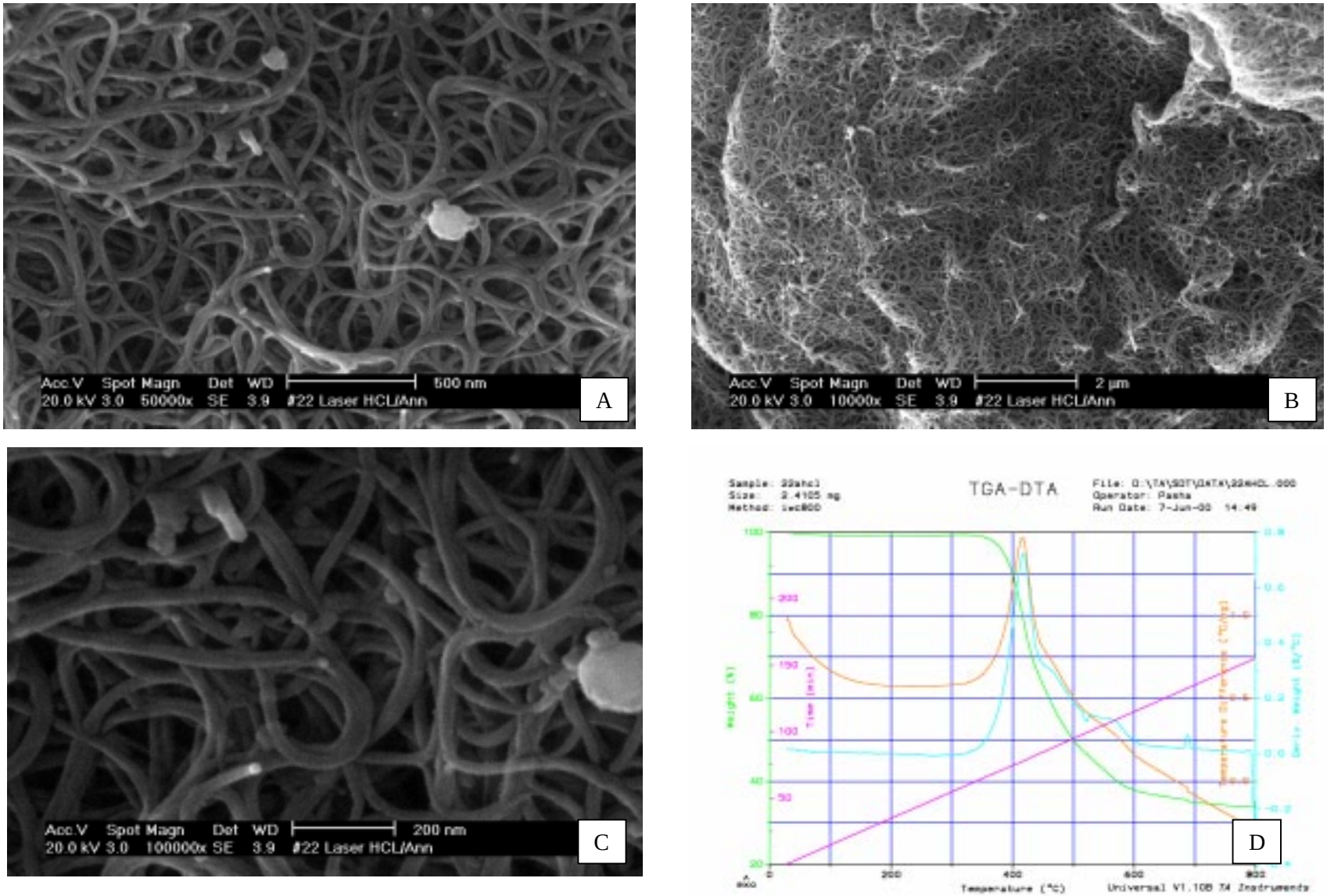

Figure 25. Sample 22 purified by solvent extraction, HCl reflux and vacuum annealing. A,B,C. SEM images at various magnifications. D. TGA data in air up to 800°C.

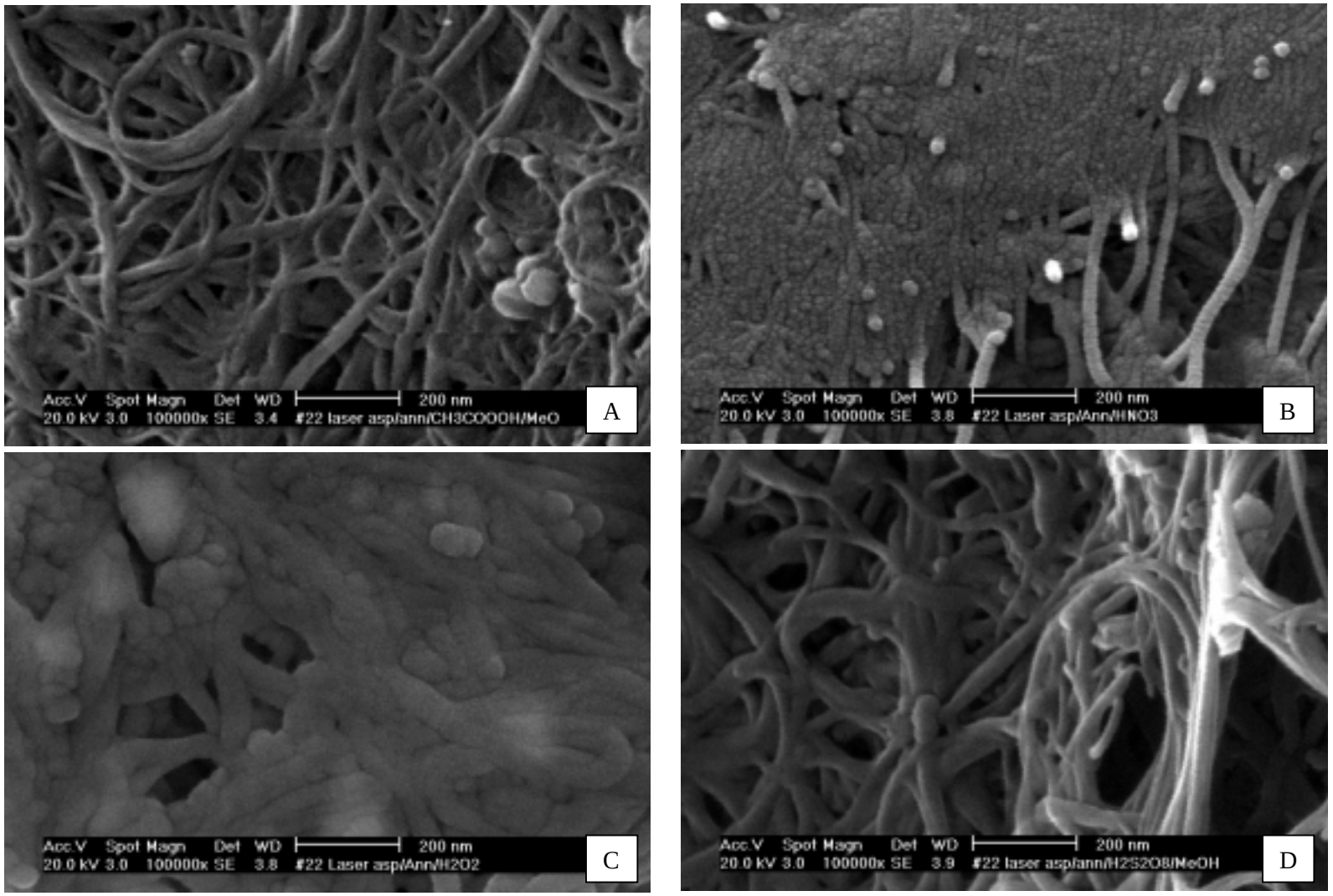

Figure 26. Laser sample #22 treated with various oxidants after vacuum annealing.
A. peroxyacetic acid (CH_3CO_cH). B. Nitric acid. C. Hydrogen peroxide. D. Persulphuric acid ($H_2S_2O_8$).

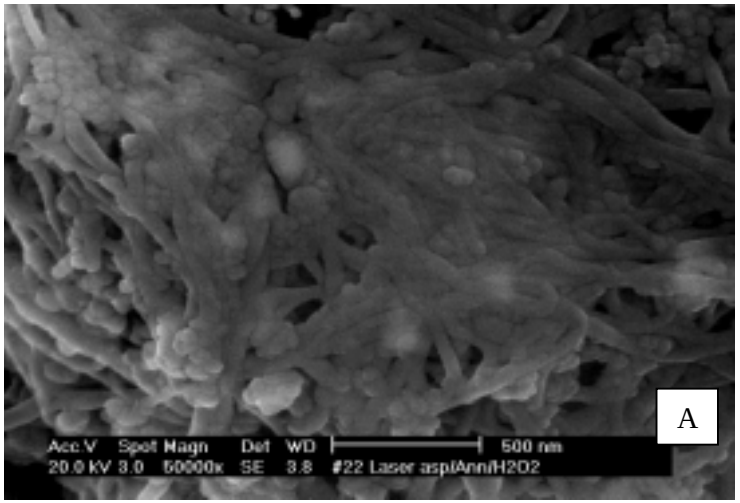

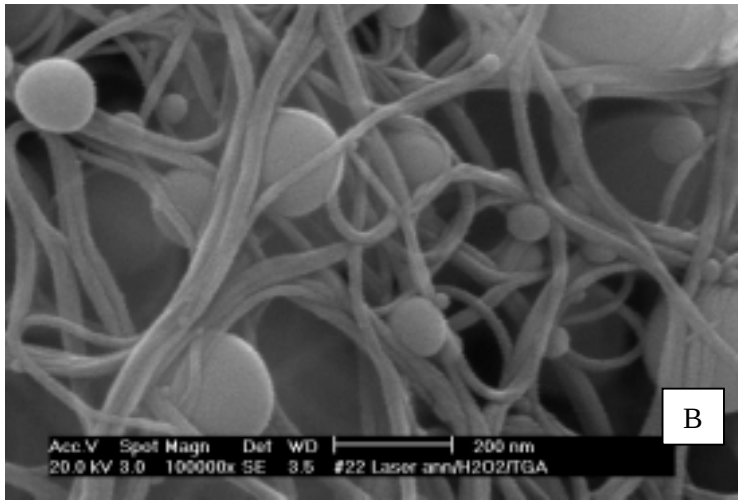

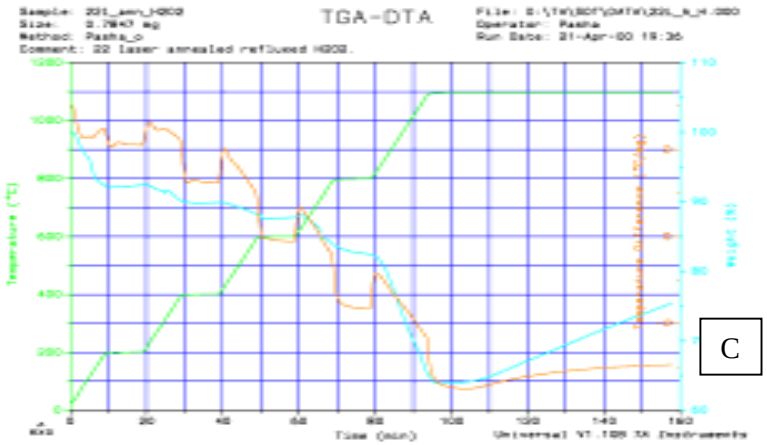

Figure 27. Sample purified by vacuum annealing + H_2O_2 reflux before and after annealing in argon up to 1100°C. A. before TGA. B. After TGA. C. TGA data in argon.

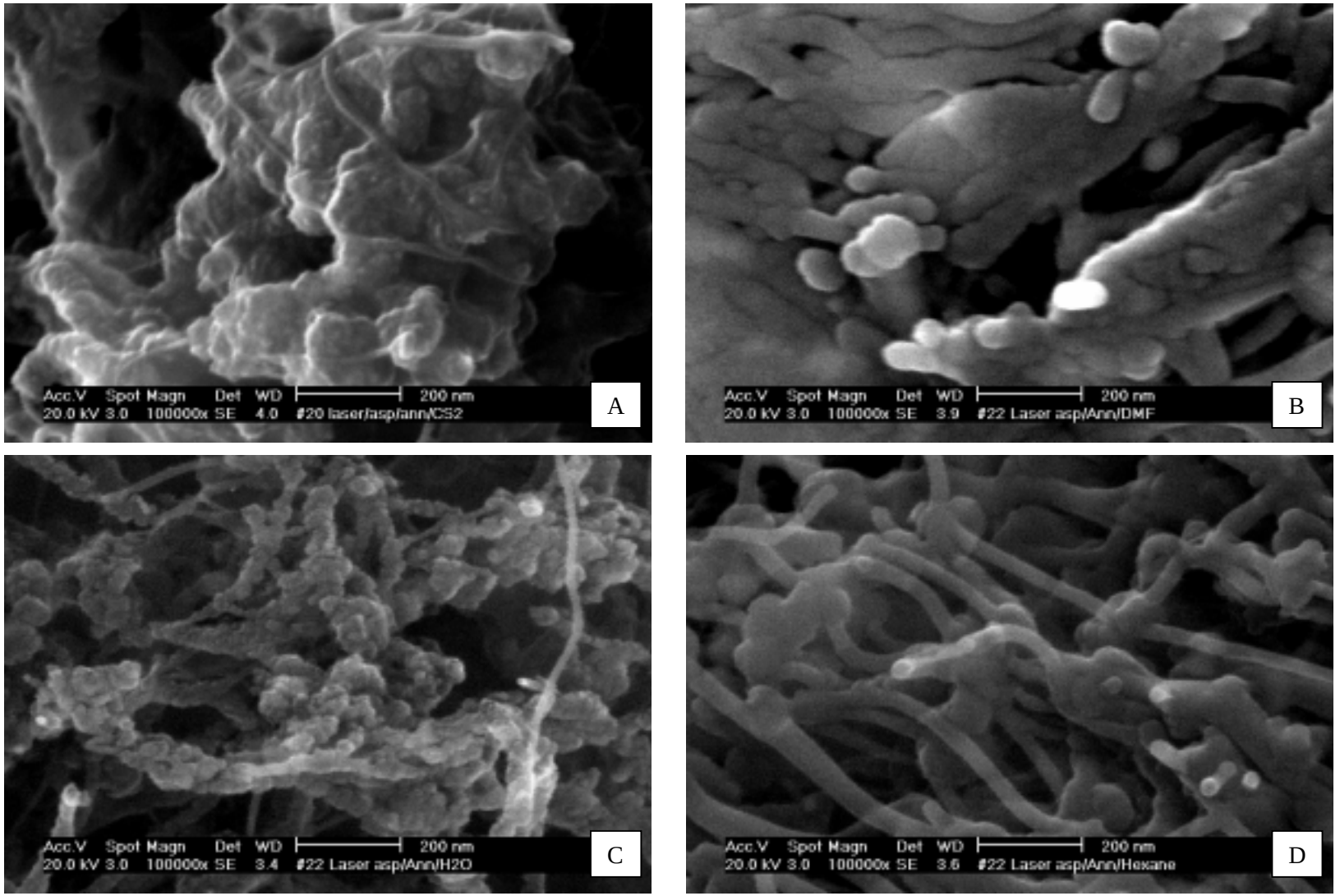

Figure 28. Laser sample #22 after vacuum annealing and subsequent dispersion in various organic solvents: A. Carbon disulfide. B. Dimethylformamide. C. Water. D. Hexane.

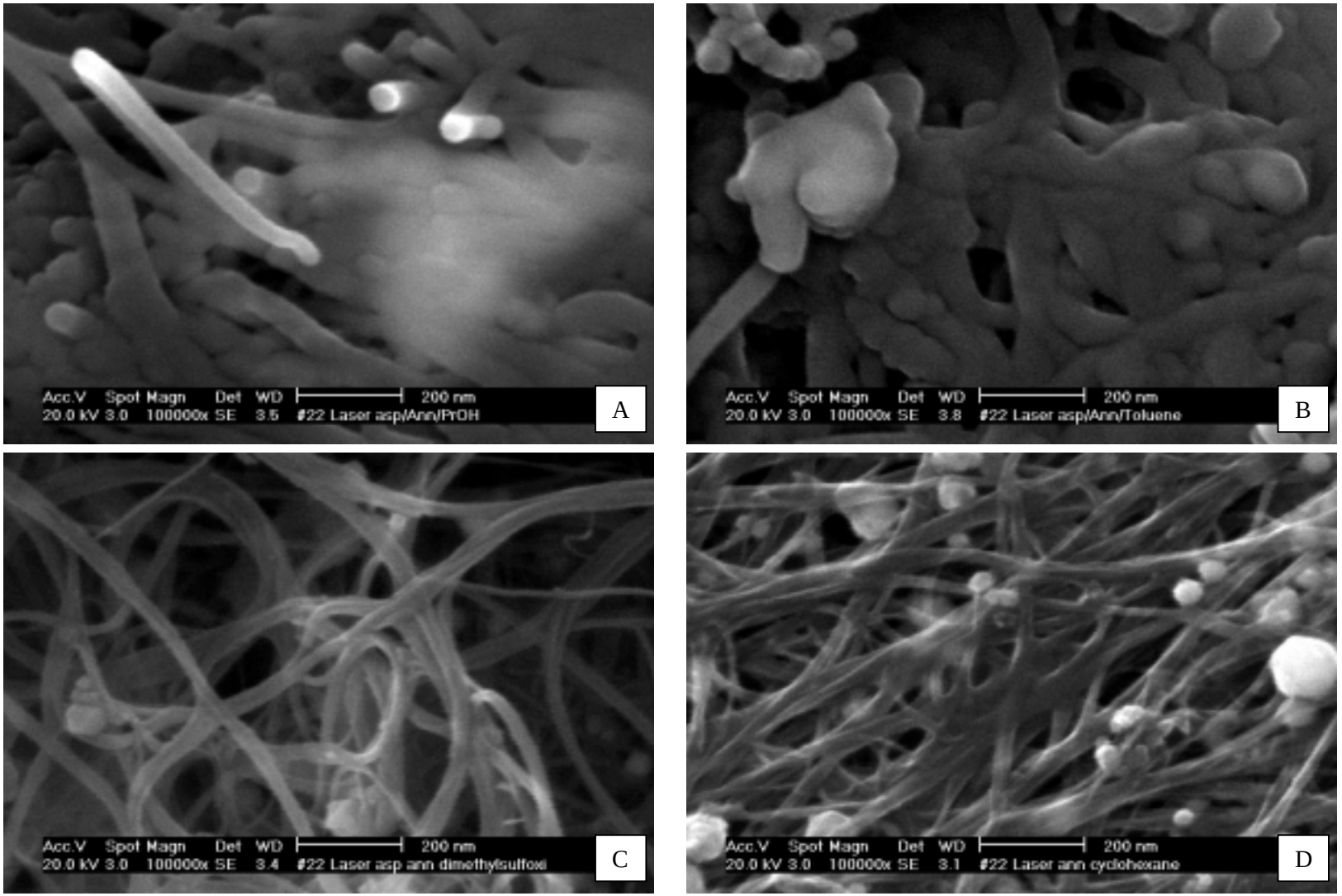

Figure 29. Laser sample #22 after vacuum annealing and subsequent dispersion in various organic solvents:
A. Propanol. B. Toluene. C. Dimetilsulfoxide. D.Cyclohexane

REPORT DOCUMENTATION PAGE	Form Approved OMB No. 0704-0188

1. AGENCY USE ONLY *(Leave Blank)*	2. REPORT DATE	3. REPORT TYPE AND DATES COVERED
	May 2001	NASA Contractor Report

4. TITLE AND SUBTITLE
Purification Procedures for Single-Wall Carbon Nanotubes

5. FUNDING NUMBERS

6. AUTHOR(S)
Olga P. Gorelik, Pavel Nikolaev, Sivaram Arepalli

7. PERFORMING ORGANIZATION NAME(S) AND ADDRESS(ES)
Lyndon B. Johnson Space Center
Houston, Texas 77058

8. PERFORMING ORGANIZATION REPORT NUMBERS
S-874

9. SPONSORING/MONITORING AGENCY NAME(S) AND ADDRESS(ES)
National Aeronautics and Space Administration
Washington, DC 20546-0001

10. SPONSORING/MONITORING AGENCY REPORT NUMBER
CR-2000-208926

11. SUPPLEMENTARY NOTES

12a. DISTRIBUTION/AVAILABILITY STATEMENT

12b. DISTRIBUTION CODE

13. ABSTRACT *(Maximum 200 words)*

This report summarizes the comparison of a variety of procedures used to purify carbon nanotubes. Carbon nanotube material is produced by the arc process and laser oven process. Most of the procedures are tested using laser-grown, single-wall nanotube (SWNT) material. The material is characterized at each step of the purification procedures by using different techniques including a scanning electron microscope (SEM), energy-dispersive X-ray spectroscopy (EDS), a transmission electron microscopy (TEM), Raman, X-ray diffractometry (XRD), a thermogravimetric analysis (TGA), nuclear magnetic resonance (NMR), and high-performance liquid chromatography (HPLC). The identified impurities are amorphous and graphitic carbon, catalyst particle aggregates, fullerenes, and hydrocarbons. Solvent extraction and low-temperature annealing are used to reduce the amount of volatile hydrocarbons and dissolve fullerenes. Metal catalysts and amorphous as well as graphitic carbon are oxidized by reflux in acids including HCl, HNO3 and HF and other oxidizers such as H2O2. High-temperature annealing in vacuum and in inert atmosphere helps to improve the quality of SWNTs by increasing crystallinity and reducing intercalation.

14. SUBJECT TERMS	15. NUMBER OF PAGES	16. PRICE CODE
carbon nanotubes; scanning electron microscope; energy-dispersive X-ray spectroscopy; transmission electron microscopy; X-ray diffractometry; thermogravimetric analysis	56	

17. SECURITY CLASSIFICATION OF REPORT	18. SECURITY CLASSIFICATION OF THIS PAGE	19. SECURITY CLASSIFICATION OF ABSTRACT	20. LIMITATION OF ABSTRACT
Unclassified	Unclassified	Unclassified	Unlimited